

CERN-PH-EP-2012-132

24 October 2012

## Measurement of prompt $J/\psi$ and beauty hadron production cross sections at mid-rapidity in pp collisions at $\sqrt{s} = 7$ TeV

The ALICE Collaboration\*

### Abstract

The ALICE experiment at the LHC has studied  $J/\psi$  production at mid-rapidity in pp collisions at  $\sqrt{s} = 7$  TeV through its electron pair decay on a data sample corresponding to an integrated luminosity  $L_{\text{int}} = 5.6 \text{ nb}^{-1}$ . The fraction of  $J/\psi$  from the decay of long-lived beauty hadrons was determined for  $J/\psi$  candidates with transverse momentum  $p_t > 1.3 \text{ GeV}/c$  and rapidity  $|y| < 0.9$ . The cross section for prompt  $J/\psi$  mesons, i.e. directly produced  $J/\psi$  and prompt decays of heavier charmonium states such as the  $\psi(2S)$  and  $\chi_c$  resonances, is  $\sigma_{\text{prompt } J/\psi}(p_t > 1.3 \text{ GeV}/c, |y| < 0.9) = 8.3 \pm 0.8 \text{ (stat.)} \pm 1.1 \text{ (syst.)} {}^{+1.5}_{-1.4} \text{ (syst. pol.)} \mu\text{b}$ . The cross section for the production of b-hadrons decaying to  $J/\psi$  with  $p_t > 1.3 \text{ GeV}/c$  and  $|y| < 0.9$  is  $\sigma_{J/\psi \leftarrow \text{hb}}(p_t > 1.3 \text{ GeV}/c, |y| < 0.9) = 1.46 \pm 0.38 \text{ (stat.)} {}^{+0.26}_{-0.32} \text{ (syst.)} \mu\text{b}$ . The results are compared to QCD model predictions. The shape of the  $p_t$  and  $y$  distributions of b-quarks predicted by perturbative QCD model calculations are used to extrapolate the measured cross section to derive the  $b\bar{b}$  pair total cross section and  $d\sigma/dy$  at mid-rapidity.

arXiv:1205.5880v2 [hep-ex] 24 Oct 2012

---

\*See Appendix A for the list of collaboration members



## 1 Introduction

The production of both charmonium mesons and beauty-flavoured hadrons, referred to as b-hadrons or  $h_B$  in this paper, in hadronic interactions represents a challenging testing ground for models based on Quantum ChromoDynamics (QCD).

The mechanisms of  $J/\psi$  production operate at the boundary of the perturbative and non-perturbative regimes of QCD. At hadron colliders,  $J/\psi$  production was extensively studied at the Tevatron [1–4] and RHIC [5]. Measurements in the new energy domain of the Large Hadron Collider (LHC) can contribute to a deeper understanding of the physics of the hadroproduction processes. The first LHC experimental results on the  $J/\psi$  transverse momentum ( $p_t$ ) differential cross sections [6–10] are well described by various theoretical approaches [11–14]. Among those results, the ALICE Collaboration reported the measurement of the rapidity ( $y$ ) and transverse momentum dependence of inclusive  $J/\psi$  production in proton–proton (pp) collisions at  $\sqrt{s} = 7$  TeV [9]. The inclusive  $J/\psi$  yield is composed of three contributions: prompt  $J/\psi$  produced directly in the proton–proton collision, prompt  $J/\psi$  produced indirectly (via the decay of heavier charmonium states such as  $\chi_c$  and  $\psi(2S)$ ), and non-prompt  $J/\psi$  from the decay of b-hadrons. Other LHC experiments have separated the prompt and non-prompt  $J/\psi$  component [6–8, 10]. However, at mid-rapidity, only the high- $p_t$  part of the differential  $d\sigma_{J/\psi}/dp_t$  distribution was measured ( $p_t > 6.5$  GeV/c), i.e. a small fraction (few percent) of the  $p_t$ -integrated cross section.

The measurement of the production of b-hadrons in pp collisions at the LHC provides a way to test, in a new energy domain, calculations of QCD processes based on the factorization approach. In this scheme, the cross sections are computed as a convolution of the parton distribution functions of the incoming protons, the partonic hard scattering cross sections, and the fragmentation functions. Measurements of cross sections for beauty quark production in high-energy hadronic interactions have been done in the past at  $p\bar{p}$  colliders at center-of-mass energies from 630 GeV [15, 16] to 1.96 TeV [2, 17–19] and in p-nucleus collisions with beam energies from 800 to 920 GeV [20]. The LHC experiments have reported measurements of b-hadron production in pp collisions at  $\sqrt{s} = 7$  TeV by studying either exclusive decays of B mesons [21–23] or semi-inclusive decays of b-hadrons [6–8, 10, 24, 25]. At mid-rapidity, the measurements are available only for  $p_t$  of the b-hadrons larger than  $\approx 5$  GeV/c, whereas the low  $p_t$  region of the differential b-hadron cross sections, where the bulk of the b-hadrons is produced, has not been studied.

In this paper, the measurement of the fraction of  $J/\psi$  from the decay of b-hadrons in pp collisions at  $\sqrt{s} = 7$  TeV for  $J/\psi$  in the ranges  $1.3 < p_t < 10$  GeV/c and  $|y| < 0.9$  is determined. This information is combined with the previous inclusive  $J/\psi$  cross section measurement reported by ALICE [9]. Prompt  $J/\psi$  and b-hadron cross sections are thus determined at mid-rapidity down to the lowest  $p_t$  reach at the LHC energy.

## 2 Experiment and data analysis

The ALICE experiment [26] consists of a central barrel, covering the pseudorapidity region  $|\eta| < 0.9$ , and a muon spectrometer with  $-4 < \eta < -2.5$  coverage. The results presented in this paper were obtained with the central barrel tracking detectors, in particular the Inner Tracking System (ITS) [26, 27] and the Time Projection Chamber (TPC) [28]. The ITS, which consists of two innermost Silicon Pixel Detector (SPD), two Silicon Drift Detector (SDD), and two outer Silicon Strip Detector (SSD) layers, provides up to six space points (hits) for each track. The TPC is a large cylindrical drift detector with an active volume that extends over the ranges  $85 < r < 247$  cm and  $-250 < z < 250$  cm in the radial and longitudinal (beam) directions, respectively. The TPC provides up to 159 space points per track and charged particle identification via specific energy loss ( $dE/dx$ ) measurement.

The event sample, corresponding to  $3.5 \times 10^8$  minimum bias events and an integrated luminosity  $L_{\text{int}} =$

$5.6\text{nb}^{-1}$ , event selection and track quality cuts used for the measurement of the inclusive  $J/\psi$  production at mid-rapidity [9] were also adopted in this analysis. In particular, an event with a reconstructed vertex position  $z_v$  was accepted if  $|z_v| < 10$  cm. The tracks were required to have a minimum  $p_t$  of  $1\text{ GeV}/c$ , a minimum number of 70 TPC space points, a  $\chi^2$  per space point of the momentum fit lower than 4, and to point back to the interaction vertex within 1 cm in the transverse plane. At least one hit in either of the two layers of the SPD was required. For tracks passing this selection, the average number of hits in the six ITS layers was 4.5–4.7, depending on the data taking period. The electron identification was based on the specific energy loss in the TPC: a  $\pm 3\sigma$  inclusion cut around the Bethe-Bloch fit for electrons and  $\pm 3.5\sigma$  ( $\pm 3\sigma$ ) exclusion cut for pions (protons) were employed [9]. Finally, electron or positron candidates compatible, together with an opposite charge candidate, with being products of  $\gamma$  conversions (the invariant mass of the pair being smaller than  $100\text{ MeV}/c^2$ ) were removed, in order to reduce the combinatorial background. It was verified, using a Monte Carlo simulation, that this procedure does not affect the  $J/\psi$  signal. In this analysis, opposite-sign (OS) electron pairs were divided in three “types”: type “first-first” ( $FF$ ) corresponds to the case when both the electron and the positron have hits in the first pixel layer, type “first-second” ( $FS$ ) are those pairs where one of them has a hit in the first layer and the other does not, while for the type “second-second” ( $SS$ ) neither of them has a hit in the first layer. The candidates of type  $SS$ , which correspond to about 10% of the total, were discarded due to the worse spatial resolution of the associated decay vertex.

A detailed description of the track and vertex reconstruction procedures can be found in [29]. The primary vertex was determined via an analytic  $\chi^2$  minimization method in which tracks are approximated as straight lines after propagation to their common point of closest approach. The vertex fit was constrained in the transverse plane using the information on the position and spread of the luminous region. The latter was determined from the distribution of primary vertices reconstructed over the run. Typically, the transverse position of the vertex has a resolution that ranges from  $40\ \mu\text{m}$  in low-multiplicity events with less than 10 charged particles per unit of rapidity to about  $10\ \mu\text{m}$  in events with a multiplicity of about 40. For each  $J/\psi$  candidate a specific primary vertex was also calculated by excluding the  $J/\psi$  decay tracks, in order to estimate a systematic uncertainty related to the evaluation of the primary vertex in the case of events with non-prompt  $J/\psi$ , as discussed in section 3. The decay vertex of the  $J/\psi$  candidate was computed with the same analytic  $\chi^2$  minimization as for the primary vertex, using the two decay tracks only and without the constraint of the luminous region.

The measurement of the fraction of the  $J/\psi$  yield coming from b-hadron decays,  $f_B$ , relies on the discrimination of  $J/\psi$  mesons produced at a distance from the pp collision vertex. The signed projection of the  $J/\psi$  flight distance onto its transverse momentum vector,  $\vec{p}_t^{J/\psi}$ , was constructed according to the formula

$$L_{xy} = \vec{L} \cdot \vec{p}_t^{J/\psi} / p_t^{J/\psi}, \quad (1)$$

where  $\vec{L}$  is the vector from the primary vertex to the  $J/\psi$  decay vertex. The variable  $x$ , referred to as “pseudoproper decay length” in the following, was introduced to separate prompt  $J/\psi$  from those produced by the decay of b-hadrons<sup>1</sup>,

$$x = \frac{c \cdot L_{xy} \cdot m_{J/\psi}}{p_t^{J/\psi}}, \quad (2)$$

where  $m_{J/\psi}$  is the (world average)  $J/\psi$  mass [30].

For events with very low  $J/\psi$   $p_t$ , the non-negligible amount of  $J/\psi$  with large opening angle between its flight direction and that of the b-hadron impairs the separation ability. Monte Carlo simulation shows

<sup>1</sup> The variable  $x$ , which was introduced in [1], mimics a similar variable used for b-hadron lifetime measurements where b-hadrons are reconstructed exclusively and therefore the mass and  $p_t$  of the b-hadron can be used in place of those of the  $J/\psi$ , to get  $c\tau = \frac{L}{\beta\gamma} = \frac{c \cdot L_{xy} \cdot M_{\text{b-hadron}}}{p_t^{\text{b-hadron}}}$ .

that the detector resolution allows the determination of the fraction of  $J/\psi$  from the decay of b-hadrons for events with  $J/\psi$   $p_t$  greater than 1.3 GeV/ $c$ .

An unbinned 2-dimensional likelihood fit was used to determine the ratio of the non-prompt to inclusive  $J/\psi$  production and the ratio of  $J/\psi$  signal candidates (the sum of both prompt and non-prompt components) to the total number of candidates,  $f_{\text{Sig}}$ , by maximizing the quantity

$$\ln L = \sum_{i=1}^N \ln F(x, m_{e^+e^-}), \quad (3)$$

where  $m_{e^+e^-}$  is the invariant mass of the electron pair and  $N$  is the total number of candidates in the range  $2.4 < m_{e^+e^-} < 4.0$  GeV/ $c^2$ . The expression for  $F(x, m_{e^+e^-})$  is

$$F(x, m_{e^+e^-}) = f_{\text{Sig}} \cdot F_{\text{Sig}}(x) \cdot M_{\text{Sig}}(m_{e^+e^-}) + (1 - f_{\text{Sig}}) \cdot F_{\text{Bkg}}(x) \cdot M_{\text{Bkg}}(m_{e^+e^-}), \quad (4)$$

where  $F_{\text{Sig}}(x)$  and  $F_{\text{Bkg}}(x)$  are Probability Density Functions (PDFs) describing the pseudoproper decay length distribution for signal and background candidates, respectively.  $M_{\text{Sig}}(m_{e^+e^-})$  and  $M_{\text{Bkg}}(m_{e^+e^-})$  are the PDFs describing the dielectron invariant mass distributions for the signal and background, respectively. A Crystal Ball function [31] is used for the former and an exponential function for the latter. The signal PDF is given by

$$F_{\text{Sig}}(x) = f'_B \cdot F_B(x) + (1 - f'_B) \cdot F_{\text{prompt}}(x), \quad (5)$$

where  $F_{\text{prompt}}(x)$  and  $F_B(x)$  are the PDFs for prompt and non-prompt  $J/\psi$ , respectively, and  $f'_B$  is the fraction of reconstructed non-prompt  $J/\psi$ ,

$$f'_B = \frac{N_{J/\psi \leftarrow \text{hB}}}{N_{J/\psi \leftarrow \text{hB}} + N_{\text{prompt} J/\psi}}, \quad (6)$$

which can differ (see below) from  $f_B$  due to different acceptance and reconstruction efficiency of prompt and non-prompt  $J/\psi$ . The distribution of non-prompt  $J/\psi$  is the convolution of the  $x$  distribution of  $J/\psi$  from b-hadron events,  $\chi_B(x)$ , and the experimental resolution on  $x$ ,  $R_{\text{type}}(x)$ , which depends on the type of candidate ( $FF$  or  $FS$ ),

$$F_B(x) = \chi_B(x') \otimes R_{\text{type}}(x' - x). \quad (7)$$

Promptly produced  $J/\psi$  mesons decay at the primary vertex, and their pseudoproper decay length distribution is thus simply described by  $R_{\text{type}}(x)$ :

$$F_{\text{prompt}}(x) = \delta(x') \otimes R_{\text{type}}(x' - x) = R_{\text{type}}(x). \quad (8)$$

The resolution function is described by the sum of two Gaussians and a power law function reflected about  $x = 0$  and was determined, as a function of the  $p_t$  of the  $J/\psi$ , with a Monte Carlo simulation study. In this simulation, which utilizes GEANT3 [32] and incorporates a detailed description of the detector material, geometry, and response, prompt  $J/\psi$  were generated with a  $p_t$  distribution extrapolated from CDF measurements [1] and a  $y$  distribution parameterization taken from Color Evaporation Model (CEM) calculations [33]. These  $J/\psi$  were individually injected into proton–proton collisions simulated using the PYTHIA 6.4.21 event generator [34, 35], and reconstructed as for  $J/\psi$  candidates in data. A data-driven method (discussed in section 3) was also developed and used to estimate the systematic uncertainty related to this procedure. The Monte Carlo  $x$  distribution of  $J/\psi$  from the decay of b-hadrons produced in proton-proton collisions simulated using the PYTHIA 6.4.21 event generator [34, 35] with Perugia-0 tuning [36] was taken as the template for the  $x$  distribution of b-hadron events in data,  $\chi_B(x)$ . A second template, used to estimate the systematic uncertainty, was obtained by decaying the simulated b-hadrons using the EvtGen package [37], and describing the final state radiation (“internal” bremsstrahlung) using PHOTOS [38, 39].

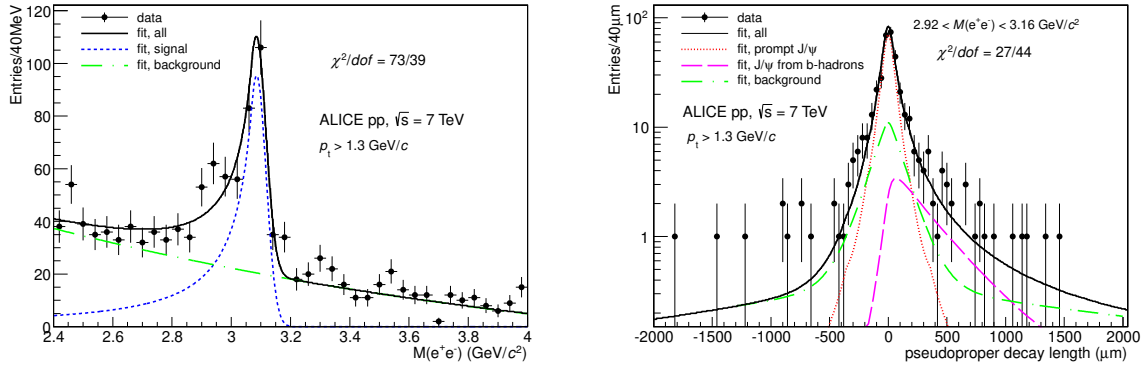


**Fig. 1:** Invariant mass (left panel) and pseudoproper decay length (right panel) distributions of opposite sign electron pairs for  $|y_{J/\psi}| < 0.9$  and  $p_t^{J/\psi} > 1.3$  GeV/c with superimposed projections of the maximum likelihood fit. The latter distribution is limited to the  $J/\psi$  candidates under the mass peak, i.e. for  $2.92 < m_{e^+e^-} < 3.16$  GeV/c<sup>2</sup>, for display purposes only. The  $\chi^2$  values of these projections are reported for both distributions.

For the background  $x$  distribution,  $F_{\text{Bkg}}(x)$ , the functional form employed by CDF [1] was used,

$$F_{\text{Bkg}}(x) = (1 - f_+ - f_- - f_{\text{sym}}) R_{\text{type}}(x) + \left[ \frac{f_+}{\lambda_+} e^{-x'/\lambda_+} \theta(x') + \frac{f_-}{\lambda_-} e^{x'/\lambda_-} \theta(-x') + \frac{f_{\text{sym}}}{2\lambda_{\text{sym}}} e^{-|x'|/\lambda_{\text{sym}}} \right] \otimes R_{\text{type}}(x' - x), \quad (9)$$

where  $\theta(x)$  is the step function,  $f_+$ ,  $f_-$  and  $f_{\text{sym}}$  are the fractions of three components with positive, negative and symmetric decay length exponential distributions, respectively. The effective parameters  $\lambda_+$ ,  $\lambda_-$  and  $\lambda_{\text{sym}}$ , and optionally also the corresponding fractions, were determined, prior to the likelihood fit maximization, with a fit to the  $x$  distribution in the sidebands of the dielectron invariant mass distribution, defined as the regions 1.8–2.6 and 3.2–5.0 GeV/c<sup>2</sup>. The introduction of these components is needed because the background consists also of random combinations of electrons from semi-leptonic decays of charm and beauty hadrons, which tend to produce positive  $x$  values, as well as of other secondary or mis-reconstructed tracks which contribute both to positive and negative  $x$  values. The first term in eq. 9, proportional to  $R_{\text{type}}(x)$ , describes the residual combinatorics of primary particles.

In figure 1 the distributions of the invariant mass and the pseudoproper decay length, the latter restricted to candidates with  $2.92 < m_{e^+e^-} < 3.16$  GeV/c<sup>2</sup>, for opposite-sign electron pairs with  $p_t > 1.3$  GeV/c are shown with superimposed projections of the maximum likelihood fit result.

The value of the fit parameter  $f'_B$  provides the fraction of non-prompt  $J/\psi$  which were reconstructed. In principle prompt and non-prompt  $J/\psi$  can have different acceptance times efficiency ( $A \times \varepsilon$ ) values. This can happen because of two effects: (i) the  $A \times \varepsilon$  depends on the  $p_t$  of the  $J/\psi$  and prompt and non-prompt  $J/\psi$  have different  $p_t$  distributions within the considered  $p_t$  range; (ii) at a given  $p_t$ , prompt and non-prompt  $J/\psi$  can have different polarization and, therefore, a different acceptance. The fraction of non-prompt  $J/\psi$ , corrected for these effects, was obtained as

$$f_B = \left( 1 + \frac{1 - f'_B}{f'_B} \cdot \frac{\langle A \times \varepsilon \rangle_B}{\langle A \times \varepsilon \rangle_{\text{prompt}}} \right)^{-1}, \quad (10)$$

where  $\langle A \times \varepsilon \rangle_B$  and  $\langle A \times \varepsilon \rangle_{\text{prompt}}$  are the average acceptance times efficiency values, in the considered  $p_t$  range and for the assumed polarization state, of non-prompt and prompt  $J/\psi$ , respectively. The acceptance times efficiency ( $A \times \varepsilon$ ) varies very smoothly with  $p_t$  and, for unpolarized  $J/\psi$  in the  $p_t$  range from 1.3 to 10 GeV/c, has a minimum of 8% at 2 GeV/c and a broad maximum of 12% at 7 GeV/c [9]. As a consequence, the  $\langle A \times \varepsilon \rangle$  values of prompt and non-prompt  $J/\psi$  differ by about 3% only in this integrated  $p_t$  range.

The central values of the resulting cross sections are quoted assuming both prompt and non-prompt  $J/\psi$  to be unpolarized and the variations due to different assumptions are estimated as a separate systematic uncertainty. The polarization of  $J/\psi$  from b-hadron decays is expected to be much smaller than for prompt  $J/\psi$  due to the averaging effect caused by the admixture of various exclusive  $B \rightarrow J/\psi + X$  decay channels. In fact, the sizeable polarization, which is observed when the polarization axis refers to the B-meson direction [40], is strongly smeared when calculated with respect to the direction of the daughter  $J/\psi$  [7], as indeed observed by CDF [2]. Therefore, these variations will be calculated in the two cases of prompt  $J/\psi$  with fully transverse ( $\lambda = 1$ ) or longitudinal ( $\lambda = -1$ ) polarization, in the Collins-Soper (CS) and helicity (HE) reference frames<sup>2</sup>, the non-prompt component being left unpolarized.

Despite the small  $J/\psi$  candidate yield, amounting to about 400 counts, the data sample could be divided into four  $p_t$  bins (1.3–3, 3–5, 5–7 and 7–10 GeV/c), and the fraction  $f_B$  was evaluated in each of them with the same technique. At low  $p_t$  the statistics is higher, but the resolution is worse and the signal over background,  $S/B$ , is smaller (i.e.  $f_{\text{sig}}$  is smaller). At high  $p_t$  the statistics is smaller, but the resolution improves and the background becomes negligible. In figure 2 the distributions of the invariant mass and of the pseudoproper decay length are shown in different  $p_t$  bins with superimposed results of the fits.

### 3 Systematic uncertainties

The different contributions to the systematic uncertainties affecting the measurement of the fraction of  $J/\psi$  from the decay of b-hadrons are discussed in the following, referring to the integrated  $p_t$  range, and summarized in table 1.

- **Resolution function.** The resolution function was determined from a Monte Carlo simulation, as discussed above. The fits were repeated by artificially modifying the resolution function, according to the formula

$$R'_{type}(x) = \frac{1}{1 + \delta} R_{type} \left( \frac{x}{1 + \delta} \right),$$

where  $\delta$  is a constant representing the desired relative variation of the RMS of the resolution function. Studies on track distance of closest approach to the primary interaction vertex in the bending plane ( $d_0$ ) show that the  $p_t$  dependence of the  $d_0$  resolution as measured in the data is reproduced within about 10% by the Monte Carlo simulation [29], but with a systematically worse resolution in data. For the  $x$  variable a similar direct comparison to data is not straightforward, however, the residual discrepancy is not expected to be larger than that observed for  $d_0$ .

The variations of  $f_B$  obtained in the likelihood fit results by varying  $\delta$  from  $-5\%$  to  $+10\%$  are  $+8\%$  and  $-15\%$ , respectively, and they were assumed as the systematic uncertainty due to this contribution.

An alternative, data-driven, approach was also considered. The  $x$  distribution of the signal, composed of prompt and non-prompt  $J/\psi$ , was obtained by subtracting the  $x$  distribution of the background, measured in the sidebands of the invariant mass distribution. This distribution is then fitted by fixing the ratio of prompt to non-prompt  $J/\psi$  to that obtained from the likelihood fit and leaving free the parameters of the resolution function. The RMS of the fitted resolution function is found to be 8% larger than the one determined using the Monte Carlo simulation, hence within the range of variation assumed for  $\delta$ .

- **Pseudoproper decay length distribution of background.** The shape of the combinatorial background was determined from a fit to the  $x$  distribution of candidates in the sidebands of the invariant mass distribution. By varying the fit parameters within their errors an envelope of distributions was

<sup>2</sup>The polar angle distribution of the  $J/\psi$  decay leptons is given by  $dN/d\cos\theta = 1 + \lambda \cos^2\theta$ .

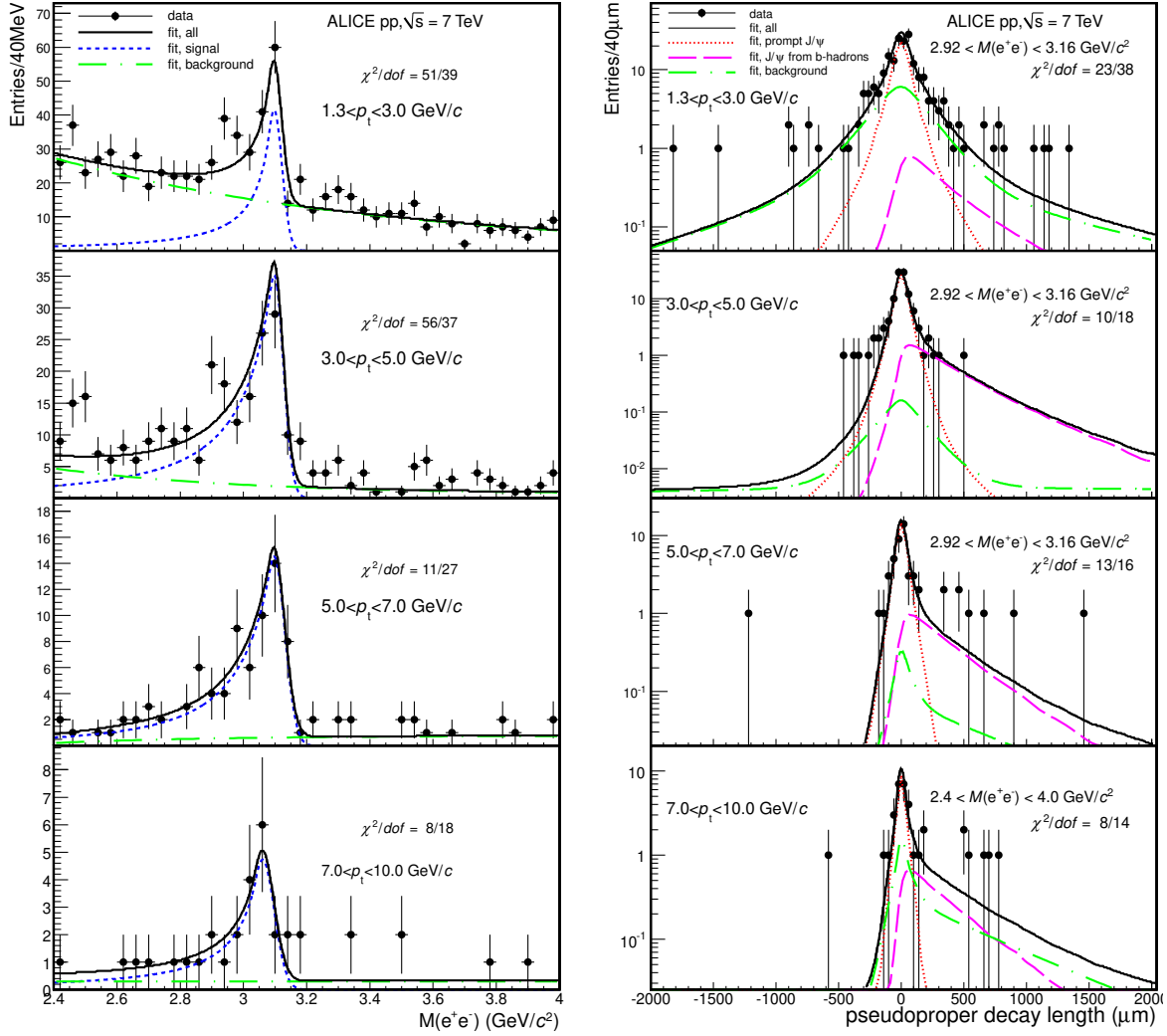


**Fig. 2:** Invariant mass (left panels) and pseudoproper decay length (right panels) distributions in different  $p_t$  bins with superimposed projections of the maximum likelihood fit. The  $\chi^2$  values of these projections are also reported for all distributions.

obtained, whose extremes were used in the likelihood fit in place of the most probable distribution. The variations in the result of the fit were determined and adopted as systematic uncertainties. Also, it was verified that the  $x$  distribution obtained for like-sign (LS) candidates, with invariant mass in the range from 2.92 to 3.16  $\text{GeV}/c^2$  complementary to the sidebands, is best fitted by a distribution which falls within the envelope of the OS distributions. Finally, the likelihood fit was repeated by relaxing, one at a time, the parameters of the functional form (eq. 9) and it was found that the values of  $f_B$  were within the estimated uncertainties. The estimated systematic uncertainty is 6%.

- **Pseudoproper decay length distribution of b-hadrons.** The fits were also done using as template for the  $x$  distribution of b-hadrons,  $\chi_B(x)$ , that obtained by the EvtGen package [37], and describing the final state radiation using PHOTOS [38,39]. The central values of the fits differ by a few percent at most and the resulting systematic uncertainty is 3%.
- **Invariant mass distributions.** The likelihood method was used in this analysis to fit simultaneously the invariant mass distribution, which is sensitive to the ratio of signal to all candidates ( $f_{\text{Sig}}$ ), and the  $x$  distribution, which determines the ratio of non-prompt to signal candidates ( $f_B$ ). The statistical uncertainties on these quantities were therefore evaluated together, including the



effects of correlations. However, the choice of the function describing the invariant mass distribution, as well as the procedure, can introduce systematic uncertainties in the evaluation of  $f_B$ . Different approaches were therefore considered: (i) the functional form describing the background was changed into an exponential plus a constant and the fit repeated; (ii) the background was described using the LS distribution and the signal was obtained by subtracting the LS from the OS distributions. The signal and the background shapes were determined with  $\chi^2$  minimizations. Both functional forms, exponential and exponential plus a constant, were considered for the background. The likelihood fit was then performed again to determine  $f_B$  (and  $f_{\text{Sig}}$ ); (iii) the same procedure as in (ii) was used, but additionally  $f_{\text{Sig}}$  was estimated *a priori* using a bin counting method [9] instead of the integrals of the best fit functions. The maximum likelihood fit was performed with  $f_{\text{Sig}}$  fixed to this new value; (iv) and (v) the same procedures as in (ii) and (iii) were used but with the background described by a track rotation (TR) method [9].

Half of the difference between the maximum and minimum  $f_B$  values obtained with the different methods was assumed as systematic uncertainty. It amounts to about 6%.

- **Primary vertex.** The effect of excluding the decay tracks of the  $J/\psi$  candidate in the computation of the primary vertex was studied with the Monte Carlo simulation: on the one hand, for the prompt  $J/\psi$ , the  $x$  resolution function is degraded, due to the fact that two prompt tracks are not used in the computation of the vertex, which is thus determined with less accuracy. The effect on the resolution is  $p_t$  dependent, with the RMS of the  $x$  distribution of prompt  $J/\psi$  increasing by 15% at low  $p_t$  and by 7% at high  $p_t$ . On the other hand, for non-prompt  $J/\psi$  a bias on the  $x$  determination should be reduced. The bias consists in an average shift of the primary vertex towards the secondary decay vertex of the b-hadrons, which is reflected in a shift of the mean of the  $x$  distribution by about  $4 \mu\text{m}$  for the  $p_t$ -integrated distribution. However, the shift is  $p_t$  and “type” dependent. In some cases the bias is observed in the opposite direction and is enhanced by removing the decay tracks of the candidate. This can happen since b-quarks are always produced in pairs. If a charged track from the fragmentation of the second b-quark also enters the acceptance, it can pull the primary vertex position towards the opposite direction. In the end, therefore, the primary vertex was computed without removing the decay tracks of the candidates. To estimate the systematic uncertainty, the analysis was repeated by either (i) removing the decay tracks in the computation of the primary vertex and using the corresponding worse resolution function in the fit or (ii) keeping those tracks and introducing an *ad hoc* shift in the distribution of the  $\chi_B(x)$ , equal to that observed in the Monte Carlo simulation for non-prompt  $J/\psi$ . The contribution to the systematic uncertainty is about 5%.
- **MC  $p_t$  spectrum.** The ratio  $\frac{\langle A \times \varepsilon \rangle_B}{\langle A \times \varepsilon \rangle_{\text{prompt}}}$  in eq. 10 was computed using MC simulations: prompt  $J/\psi$  were generated with the  $p_t$  distribution extrapolated from CDF measurements [1] and the  $y$  distribution parameterized from CEM [33]; b-hadrons were generated using the PYTHIA 6.4.21 [34,35] event generator with Perugia-0 tuning [36]. By varying the average  $p_t$  of the  $J/\psi$  distributions within a factor 2, a 1.5% variation in the acceptance was obtained both for prompt and non-prompt  $J/\psi$ . Such a small value is a consequence of the weak  $p_t$  dependence of the acceptance. For the measurement integrated over  $p_t$  ( $p_t > 1.3 \text{ GeV}/c$ ), the  $A \times \varepsilon$  values of prompt and non-prompt  $J/\psi$  differ by about 3% only. The uncertainty due to Monte Carlo  $p_t$  distributions is thus estimated to be 1%. When estimating  $f_B$  in  $p_t$  bins, this uncertainty is negligible.
- **Polarization.** The variations of  $f_B$  obtained assuming different polarization scenarios for the prompt component only were evaluated, as discussed in section 2, and are reported in table 1. The maximum variations are quoted as separate errors.

The study of systematic uncertainties was repeated as a function of  $p_t$ . In table 1 the results are summarized for the integrated  $p_t$  range ( $p_t > 1.3 \text{ GeV}/c$ ) and for the lowest (1.3–3  $\text{GeV}/c$ ) and highest

**Table 1:** Systematic uncertainties (in percent) on the measurement of the fraction of  $J/\psi$  from the decay of b-hadrons,  $f_B$ . The variations of  $f_B$  are also reported, with respect to the case of both prompt and non-prompt  $J/\psi$  unpolarized, when assuming the prompt component with given polarization.

Source	Systematic uncertainty (%)		
	$p_t$ integrated	lowest $p_t$ bin	highest $p_t$ bin
Resolution function	+8, -15	+15, -25	+2, -3
$x$ distribution of background	$\pm 6$	$\pm 13$	$\pm 1$
$x$ distribution of b-hadrons	$\pm 3$	$\pm 3$	$\pm 2$
$m_{e^+e^-}$ distributions	$\pm 6$	$\pm 11$	$\pm 4$
Primary vertex	+4, -5	$\pm 4$	+4, -8
MC $p_t$ spectrum	$\pm 1$	0	0
Total	+12, -18	+23, -30	+6, -9
Polarization (prompt $J/\psi$ )			
CS ( $\lambda = -1$ )	+13	+22	+5
CS ( $\lambda = +1$ )	-10	-19	-3
HE ( $\lambda = -1$ )	+17	+19	+11
HE ( $\lambda = +1$ )	-14	-16	-8

(7–10 GeV/c)  $p_t$  bins. All systematic uncertainties increase with decreasing  $p_t$ , except the one related to the primary vertex measurement.

## 4 Results

### 4.1 Fraction of $J/\psi$ from the decay of b-hadrons

The fraction of  $J/\psi$  from the decay of b-hadrons in the experimentally accessible kinematic range,  $p_t > 1.3$  GeV/c and  $|y| < 0.9$ , which is referred to as “measured region” in the following, is

$$f_B = 0.149 \pm 0.037 (\text{stat.})^{+0.018}_{-0.027} (\text{syst.})^{+0.025(\lambda_{\text{HE}}=1)}_{-0.021(\lambda_{\text{HE}}=-1)} (\text{syst.pol.}).$$

The fractions measured in the  $p_t$  bins are reported in table 2 and shown in figure 3. In the figure, the data symbols are placed at the average value of the  $p_t$  distribution of each bin. The average was computed using the above mentioned Monte Carlo distributions: the one based on the CDF extrapolation [33] and that using PYTHIA [34, 35] with Perugia-0 tuning [36] for prompt and non-prompt  $J/\psi$ , respectively, weighted by the measured  $f_B$ . In figure 3 the results of the ATLAS [8] and CMS [10] experiments measured at mid-rapidity for the same colliding system are also shown. The ALICE results extend the mid-rapidity measurements down to low  $p_t$ .

### 4.2 Prompt $J/\psi$ production

By combining the measurement of the inclusive  $J/\psi$  cross section, which was determined as described in [9], and the  $f_B$  value, the prompt  $J/\psi$  cross section was obtained:

$$\sigma_{\text{prompt } J/\psi} = (1 - f_B) \cdot \sigma_{J/\psi}. \quad (11)$$

The numerical values of the inclusive  $J/\psi$  cross section in the  $p_t$  ranges used for this analysis are summarized in table 2. In the measured region the integrated cross section is  $\sigma_{\text{prompt } J/\psi}(|y| < 0.9, p_t > 1.3 \text{ GeV}/c) = 8.3 \pm 0.8(\text{stat.}) \pm 1.1(\text{syst.})^{+1.5(\lambda_{\text{HE}}=1)}_{-1.4(\lambda_{\text{HE}}=-1)} \mu\text{b}$ . The systematic uncertainties related to the unknown polarization are quoted for the reference frame where they are the largest.

The differential distribution  $\frac{d^2\sigma_{\text{prompt } J/\psi}}{dp_t dy}$  is shown as a function of  $p_t$  in figure 4 and  $\frac{d\sigma_{\text{prompt } J/\psi}}{dy}$  is plotted in figure 5. The numerical values are summarized in table 2. In figure 4 the statistical and all systematic

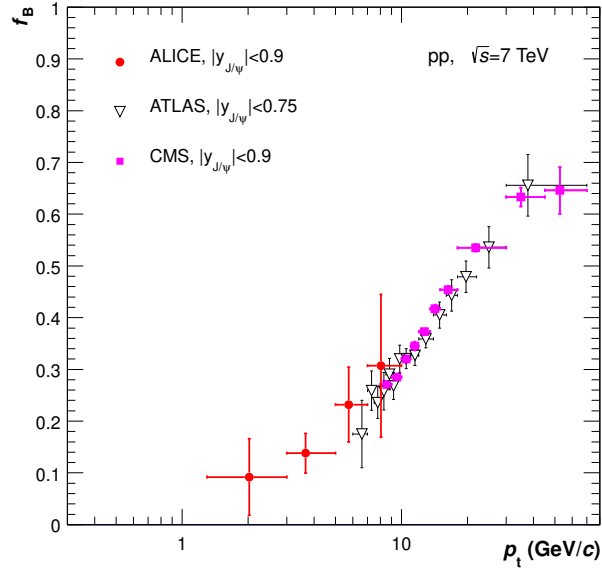


**Fig. 3:** The fraction of  $J/\psi$  from the decay of  $b$ -hadrons as a function of  $p_t$  of  $J/\psi$  compared with results from ATLAS [8] and CMS [10] in pp collisions at  $\sqrt{s}=7$  TeV.

errors are added in quadrature for better visibility, while in figure 5 the error bar shows the quadratic sum of statistical and systematic errors, except for the 3.5% systematic uncertainty on luminosity and the 1% on the branching ratio ( $BR$ ), which are added in quadrature and shown as box. The results shown in figures 4 and 5 assume unpolarized  $J/\psi$  production. Systematic uncertainties due to the unknown  $J/\psi$  polarization are not shown. Results by the CMS [6, 10], LHCb [7] and ATLAS [8] Collaborations are shown for comparison. Also for these data the uncertainties due to luminosity and to the  $BR$  are shown separately (boxes) in figure 5, while the error bars represent the statistical and the other sources of systematic uncertainties added in quadrature.

The ALICE  $\frac{d^2\sigma_{\text{prompt } J/\psi}}{dy dp_t}$  measurement at mid-rapidity (left panel of figure 4) is complementary to the data of CMS, available for  $|y| < 0.9$  and  $p_t > 8$  GeV/ $c$ , and ATLAS, which covers the region  $|y| < 0.75$  and  $p_t > 7$  GeV/ $c$ . In the right panel of figure 4, the ALICE results are compared to next-to-leading order (NLO) non-relativistic QCD (NRQCD) theoretical calculations by M. Butenschön and B.A. Kniehl [12] and Y.-Q. Ma et al. [13]. Both calculations include color-singlet (CS), color-octet (CO), and heavier charmonium feed-down contributions. For one of the two models (M. Butenschön and B.A. Kniehl) the partial results with only the CS contribution are also shown. The comparison suggests that the CO processes are indispensable to describe the data also at low  $p_t$ . The results are also compared to the model of V.A. Saleev et al. [14], which includes the contribution of partonic sub-processes involving  $t$ -channel parton exchanges and provides a prediction down to  $p_t = 0$ .

The ALICE result for  $\frac{d\sigma_{\text{prompt } J/\psi}}{dy}$  (figure 5), which equals

$$\frac{d\sigma_{\text{prompt } J/\psi}}{dy} = 5.89 \pm 0.60(\text{stat.})_{-0.90}^{+0.88}(\text{syst.})_{-0.01}^{+0.03}(\text{extr.})_{-0.99}^{+1.01}(\lambda_{\text{HE}}=1)_{-0.99}^{+1.01}(\lambda_{\text{HE}}=-1) \mu\text{b},$$

was obtained by subtracting from the inclusive  $J/\psi$  cross section measured for  $p_t > 0$  that of  $J/\psi$  coming from  $b$ -hadron decays. The latter was determined, as discussed in the next section, by extrapolating the cross section from the measured region down to  $p_t > 0$  using an implementation of pQCD calculations at fixed order with next-to leading-log resummation (FONLL) [41]. The extrapolation uncertainty is negligible with respect to the other systematic uncertainties. In figure 5 the CMS and LHCb results for

**Table 2:** The fraction of  $J/\psi$  from the decay of b-hadrons and cross sections. Some of the contributions to the systematic uncertainty do not depend on  $p_t$ , thus affecting only the overall normalization, and they are separately quoted (correl.). The contributions which depend on  $p_t$ , even when they are correlated bin by bin, were included among the non-correlated systematic errors. The values of  $\langle p_t \rangle$  were computed using Monte Carlo distributions (see text for details).

$p_t$ (GeV/c)	$\langle p_t \rangle$ (GeV/c)	Measured quantity	Systematic uncertainties				
			Correl.	Non-correl.	Extrap.	Polariz., CS	Polariz., HE
$f_B$ (%)							
1.3–3.0	2.02	$9.2 \pm 7.4$	0	+2.1, –2.8	0	+2.0, –1.7	+1.7, –1.5
3.0–5.0	3.65	$13.8 \pm 3.8$	0	+1.5, –2.1	0	+1.3, –1.0	+2.1, –3.0
5.0–7.0	5.75	$23.2 \pm 7.2$	0	+1.6, –2.1	0	+0.2, –0.2	+3.5, –2.6
7.0–10.0	8.06	$30.7 \pm 13.8$	0	+1.8, –2.8	0	+1.5, –0.9	+3.4, –2.5
$p_t > 1.3$	2.85	$14.9 \pm 3.7$	0	+1.8, –2.7	0	+1.9, –1.5	+2.5, –2.1
$p_t > 0$	2.41	$14.3 \pm 3.6$	0	+1.8, –2.6	+0.2, –0.5	+2.4, –1.6	+2.5, –1.9
$d^2\sigma_{J/\psi}/dydp_t$ ( $\frac{nb}{GeV/c}$ )							
1.3–3.0	2.02	$1780 \pm 210$	$\pm 65$	$\pm 250$	0	+400, –320	+330, –280
3.0–5.0	3.65	$715 \pm 125$	$\pm 25$	$\pm 90$	0	+50, –60	+170, –90
5.0–7.0	5.74	$405 \pm 70$	$\pm 15$	$\pm 45$	0	+1, –3	+50, –50
7.0–10.0	8.06	$60 \pm 25$	$\pm 2$	$\pm 12$	0	+2, –3	+5, –6
$d^2\sigma_{\text{prompt } J/\psi}/dydp_t$ ( $\frac{nb}{GeV/c}$ )							
1.3–3.0	2.02	$1600 \pm 230$	$\pm 60$	$\pm 230$	0	+400, –320	+330, –280
3.0–5.0	3.65	$620 \pm 110$	$\pm 20$	$\pm 80$	0	+50, –60	+170, –90
5.0–7.0	5.74	$310 \pm 60$	$\pm 10$	$\pm 35$	0	+1, –3	+50, –50
7.0–10.0	8.03	$40 \pm 18$	$\pm 1$	$\pm 8$	0	+2, –3	+5, –6
$\sigma_{\text{prompt } J/\psi}( y_{J/\psi}  < 0.9)$ ( $\mu\text{b}$ )							
$p_t > 1.3$	2.81	$8.3 \pm 0.8$		$\pm 1.1$	0	+1.0, –1.2	+1.5, –1.4
$p_t > 0$	2.37	$10.6 \pm 1.1$		$\pm 1.6$	+0.06, –0.02	+1.6, –1.7	+1.9, –1.8
$\sigma_{J/\psi \leftarrow \text{hB}}( y_{J/\psi}  < 0.9)$ ( $\mu\text{b}$ )							
$p_t > 1.3$	3.07	$1.46 \pm 0.38$		+0.26, –0.32	0	0	0
$p_t > 0$	2.62	$1.77 \pm 0.46$		+0.32, –0.39	+0.02, –0.06	0	0
$d\sigma_{b\bar{b}}/dy _{ y  < 0.9}$ ( $\mu\text{b}$ )							
		$43 \pm 11$		+9, –10	+0.6, –1.5	0	0
$\sigma_{b\bar{b}}$ ( $\mu\text{b}$ )							
		$282 \pm 74$		+58, –68	+8, –7	0	0

the rapidity bins where the  $p_t$  coverage extends down to zero were selected. For CMS, the value for  $1.6 < |y| < 2.4$  was obtained by integrating the published  $d^2\sigma_{\text{prompt } J/\psi}/dp_t dy$  data [6]. The ALICE data point at mid-rapidity complements the other LHC measurements of prompt  $J/\psi$  production cross section as a function of rapidity. It is worth noting that the uncertainties of the data sets of the three experiments are uncorrelated, except for that (negligible) of the  $BR$ , while within the same experiment most of the systematic uncertainties are correlated. The prediction of the model by V.A. Saleev et al. [14] at mid-rapidity provides  $\frac{d\sigma_{\text{prompt } J/\psi}}{dy} = 7.8^{+9.7}_{-4.5} \mu\text{b}$ , which, within the large band of theoretical uncertainties, is in agreement with our measurement.

### 4.3 Beauty hadron production

The cross section of  $J/\psi$  from b-hadrons decay was obtained as  $\sigma_{J/\psi \leftarrow \text{hB}} = f_B \cdot \sigma_{J/\psi}$ . In the measured region it is

$$\sigma_{J/\psi \leftarrow \text{hB}}(p_t > 1.3 \text{ GeV}/c, |y| < 0.9) = 1.46 \pm 0.38(\text{stat.})^{+0.26}_{-0.32}(\text{syst.}) \mu\text{b}.$$

This measurement can be compared to theoretical calculations based on the factorization approach. In particular, the prediction of the FONLL [41], which describes well the beauty production at Tevatron energy, provides [42]  $1.33^{+0.59}_{-0.48} \mu\text{b}$ , in good agreement with the measurement. For this calculation CTEQ6.6 parton distribution functions [43] were used and the theoretical uncertainty was obtained by varying the factorization and renormalization scales,  $\mu_F$  and  $\mu_R$ , independently in the ranges  $0.5 < \mu_F/m_t < 2$ ,

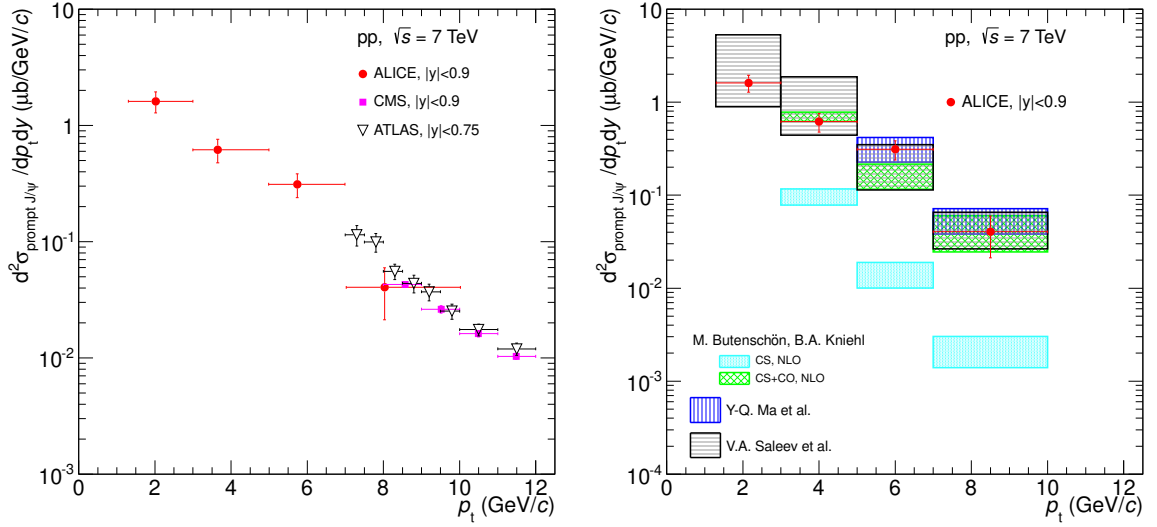


**Fig. 4:**  $\frac{d^2\sigma_{\text{prompt } J/\psi}}{dp_t dy}$  as a function of  $p_t$  compared to results from ATLAS [8] and CMS [10] at mid-rapidity (left panel) and to theoretical calculations [12–14] (right panel). The error bars represent the quadratic sum of the statistical and systematic uncertainties.

$0.5 < \mu_R/m_t < 2$ , with the constraint  $0.5 < \mu_F/\mu_R < 2$ , where  $m_t = \sqrt{p_t^2 + m_b^2}$ . The beauty quark mass was varied within  $4.5 < m_b < 5.0$  GeV/ $c^2$ .

The same FONLL calculations were used to extrapolate the cross section of non-prompt  $J/\psi$  down to  $p_t$  equal to zero. The extrapolation factor, which is equal to  $1.212_{-0.038}^{+0.016}$ , was computed as the ratio of the cross section for  $p_t^{J/\psi} > 0$  and  $|y_{J/\psi}| < 0.9$  to that in the measured region ( $p_t^{J/\psi} > 1.3$  GeV/ $c$  and  $|y_{J/\psi}| < 0.9$ ). Using the PYTHIA event generator with Perugia-0 tuning instead of FONLL provides an extrapolation factor of 1.156. The measured cross section corresponds thus to about 80% of the  $p_t$ -integrated cross section at mid-rapidity. Dividing by the rapidity range  $\Delta y = 1.8$  one obtains

$$\frac{d\sigma_{J/\psi \leftarrow h_B}}{dy} = 0.98 \pm 0.26 (\text{stat.})_{-0.22}^{+0.18} (\text{syst.})_{-0.03}^{+0.01} (\text{extr.}) \mu\text{b}.$$

In figure 6 this measurement is plotted together with the LHCb [7] and CMS [6] data at forward rapidity. For CMS the values for  $1.2 < |y| < 1.6$  and  $1.6 < |y| < 2.4$  were obtained by integrating the published  $d^2\sigma_{J/\psi \leftarrow h_B}/dp_t dy$  data [6]; the value for  $1.2 < |y| < 1.6$  was also extrapolated from  $p_t^{\text{min}} = 2.0$  GeV/ $c$  to  $p_t = 0$ , with the approach based on the FONLL calculations as previously described. The extrapolation uncertainties are shown in figure 6 as the slashed areas. The central FONLL prediction and its uncertainty band are also shown. A good agreement between data and theory is observed.

A similar procedure was used to derive the  $b\bar{b}$  quark-pair production cross section

$$\frac{d\sigma_{b\bar{b}}}{dy} = \frac{d\sigma_{b\bar{b}}^{\text{theory}}}{dy} \times \frac{\sigma_{J/\psi \leftarrow h_B}(p_t^{J/\psi} > 1.3 \text{ GeV}/c, |y_{J/\psi}| < 0.9)}{\sigma_{J/\psi \leftarrow h_B}^{\text{theory}}(p_t^{J/\psi} > 1.3 \text{ GeV}/c, |y_{J/\psi}| < 0.9)}, \quad (12)$$

where the average branching fraction of inclusive b-hadron decays to  $J/\psi$  measured at LEP [44–46],  $BR(h_b \rightarrow J/\psi + X) = (1.16 \pm 0.10)\%$ , was used in the computation of  $\sigma_{J/\psi \leftarrow h_B}^{\text{theory}}$ . The extrapolation with the FONLL calculations provides

$$\frac{d\sigma_{b\bar{b}}}{dy} = 43 \pm 11 (\text{stat.})_{-10}^{+9} (\text{syst.})_{-1.5}^{+0.6} (\text{extr.}) \mu\text{b}.$$

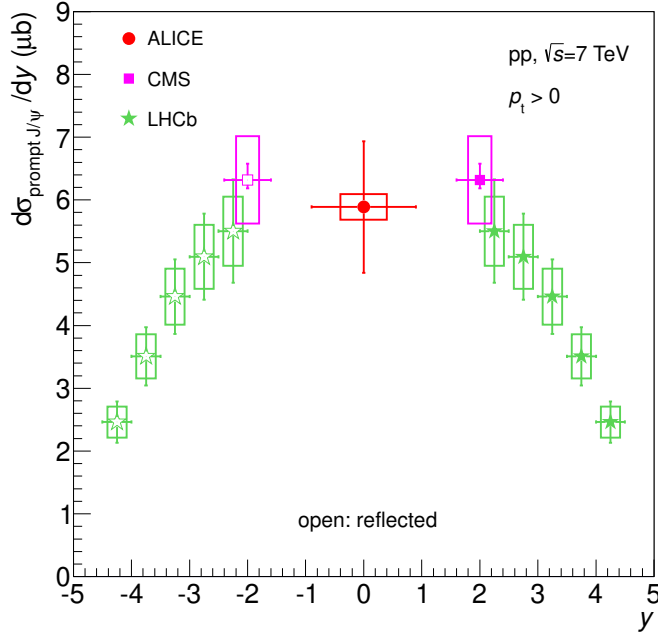


**Fig. 5:**  $\frac{d\sigma_{\text{prompt } J/\psi}}{dy}$  as a function of  $y$ . The error bars represent the quadratic sum of the statistical and systematic errors, while the systematic uncertainties on luminosity and branching ratio are shown as boxes around the data points. The symbols are plotted at the center of each bin. The CMS value was obtained by integrating the published  $d^2\sigma_{\text{prompt } J/\psi}/dp_t dy$  data measured for  $1.6 < |y| < 2.4$  [6]. The results obtained by LHCb [7] and CMS are reflected with respect to  $y = 0$  (open symbols).

Using the PYTHIA event generator with Perugia-0 tuning (with the EvtGen package to describe the particle decays) instead of FONLL results in a central value of  $40.4$  ( $40.9$ )  $\mu\text{b}$ . A compilation of measurements of  $d\sigma_{b\bar{b}}/dy$  at mid-rapidity is plotted in figure 7 as a function of  $\sqrt{s}$ , with superimposed FONLL predictions.

Finally, the total  $b\bar{b}$  cross section was obtained as

$$\sigma(\text{pp} \rightarrow b\bar{b} + X) = \alpha_{4\pi} \frac{\sigma_{J/\psi \leftarrow h_B}(p_t^{J/\psi} > 1.3 \text{ GeV}/c, |y_{J/\psi}| < 0.9)}{2 \cdot BR(h_b \rightarrow J/\psi + X)}, \quad (13)$$

where  $\alpha_{4\pi}$  is the ratio between the yield of  $J/\psi$  mesons (from the decay of b-hadrons) in the full phase space and the yield in the measured region  $|y_{J/\psi}| < 0.9$  and  $p_t^{J/\psi} > 1.3 \text{ GeV}/c$ . The FONLL calculations provide  $\alpha_{4\pi} = 4.49_{-0.10}^{+0.12}$ , which produces  $\sigma(\text{pp} \rightarrow b\bar{b} + X) = 282 \pm 74(\text{stat.})_{-68}^{+58}(\text{syst.})_{-7}^{+8}(\text{extr.}) \mu\text{b}$ . The extrapolation factor  $\alpha_{4\pi}$  was also estimated using PYTHIA with Perugia-0 tuning and found to be  $\alpha_{4\pi}^{\text{PYTHIA}} = 4.20$ . This measurement is in good agreement with those of the LHCb experiment, namely  $288 \pm 4(\text{stat.}) \pm 48(\text{syst.}) \mu\text{b}$  and  $284 \pm 20(\text{stat.}) \pm 49(\text{syst.}) \mu\text{b}$ , which were based on the measured cross sections determined in the forward rapidity range from b-hadron decays into  $J/\psi X$  and  $D^0 \mu \nu X$ , respectively [7, 24].

## 5 Summary

Results on the production cross section of prompt  $J/\psi$  and  $J/\psi$  from the decay of b-hadrons at mid-rapidity in pp collisions at  $\sqrt{s} = 7 \text{ TeV}$  have been presented. The measured cross sections have been compared to theoretical predictions based on QCD and results from other experiments. Prompt  $J/\psi$  production is well described by NLO NRQCD models that include color-octet processes. The cross

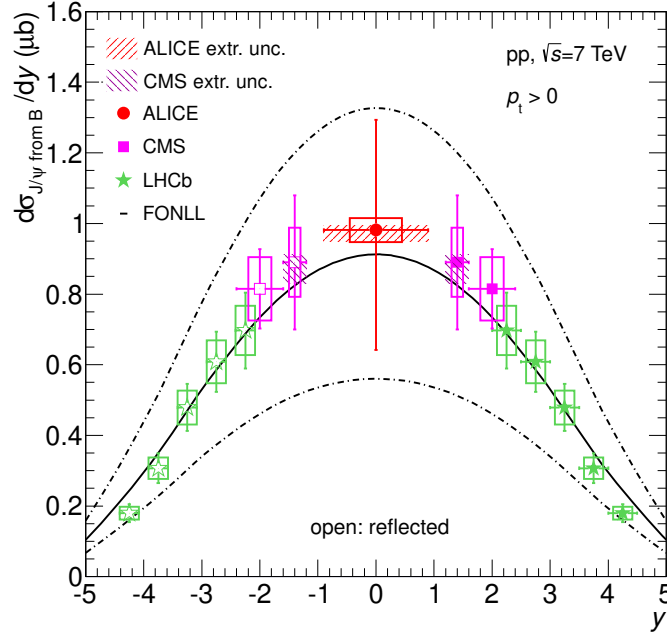


**Fig. 6:**  $\frac{d\sigma_{J/\psi \text{ from B}}}{dy}$  as a function of  $y$ . The error bars represent the quadratic sum of the statistical and systematic errors, while the systematic uncertainties on luminosity and branching ratio are shown as boxes. The systematic uncertainties on the extrapolation to  $p_t = 0$  are indicated by the slashed areas. The CMS values were obtained by integrating the published  $d^2\sigma_{J/\psi \text{ from B}}/dp_t dy$  data measured for  $1.2 < |y| < 1.6$  and  $1.6 < |y| < 2.4$  [6]. The results obtained in the forward region by LHCb [7] are reflected with respect to  $y = 0$  (open symbols). The FONLL calculation [41, 42] (and its uncertainty) is represented by solid (dashed) lines.

section of  $J/\psi$  from b-hadron decays is in good agreement with the FONLL prediction, based on perturbative QCD. The ALICE results at mid-rapidity, covering a lower  $p_t$  region down to  $p_t = 1.3$  GeV/c, are complementary to those of the ATLAS and CMS experiments, which are available for  $J/\psi$   $p_t$  above 6.5 GeV/c. Using the shape of the  $p_t$  and  $y$  distributions of b-quarks predicted by FONLL calculations, the mid-rapidity  $d\sigma/dy$  and the total production cross section of  $b\bar{b}$  pairs were determined.

## References

- [1] D. Acosta et al. (CDF Collaboration), Phys. Rev. **D71**, 032001 (2005).
- [2] A. Abulencia et al. (CDF Collaboration), Phys. Rev. Lett. **99**, 132001 (2007).
- [3] S. Abachi et al. (D0 Collaboration), Phys. Lett. **B370**, 239 (1996).
- [4] B. Abbott et al. (D0 Collaboration), Phys. Rev. Lett. **82**, 35 (1999).
- [5] A. Adare et al. (PHENIX Collaboration), Phys. Rev. Lett. **98**, 232002 (2007).
- [6] V. Khachatryan et al. (CMS Collaboration), Eur. Phys. J. **C71**, 1575 (2011).
- [7] R. Aaij et al. (LHCb Collaboration), Eur. Phys. J. **C71**, 1645 (2011).
- [8] G. Aad et al. (ATLAS Collaboration), Nucl. Phys. **B850**, 387 (2011).
- [9] K. Aamodt et al. (ALICE Collaboration), Phys. Lett. **B704**, 442 (2011); *ibidem*, Erratum *in press*.
- [10] S. Chatrchyan et al. (CMS Collaboration), J. High Energy Phys. **2**, 011 (2012).
- [11] J.P. Lansberg, Eur. Phys. J. **C 61**, 693(2009).
- [12] M. Butenschön and B.A. Kniehl, Phys. Rev. Lett. **106**, 022003 (2011).
- [13] Y.-Q. Ma, K. Wang, K.T. Chao, Phys. Rev. Lett. **106**, 042002 (2011).

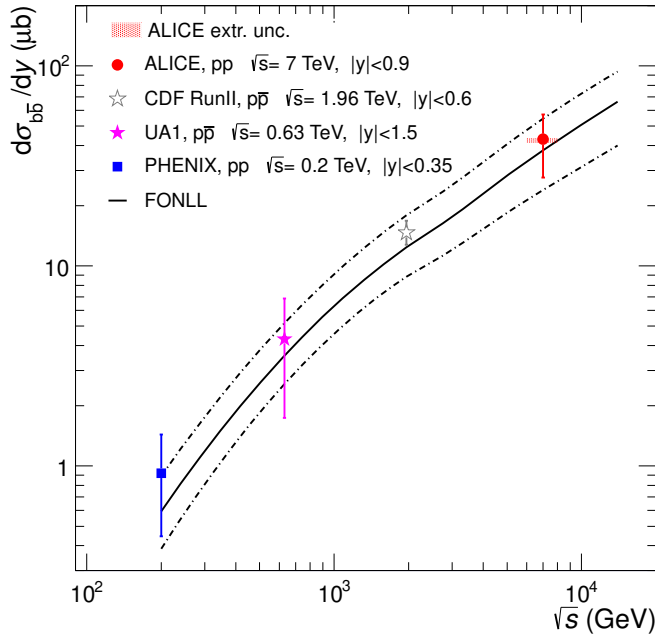


**Fig. 7:**  $d\sigma_{b\bar{b}}/dy$  at mid rapidity as a function of  $\sqrt{s}$  in pp (PHENIX [47] and ALICE results) and  $p\bar{p}$  (UA1 [16] and CDF [17] results) collisions. The FONLL calculation [41,42] (and its uncertainty) is represented by solid (dashed) lines.

- [14] V.A. Saleev, M.A. Nefedov and A.V. Shipilova, Phys. Rev. **D 85**, 074013 (2012).
- [15] C. Albajar et al. (UA1 Collaboration), Phys. Lett. **B 213**, 405 (1988).
- [16] C. Albajar et al. (UA1 Collaboration), Phys. Lett. **B 256**, 121 (1991).
- [17] F. Abe et al. (CDF Collaboration), Phys. Rev. Lett. **75**, 1451 (1995).
- [18] S. Abachi et al. (D0 Collaboration), Phys. Rev. Lett. **74**, 3548 (1995).
- [19] D. Acosta et al. (CDF Collaboration), Phys. Rev. **D65**, 052005 (2002).
- [20] Y.M. Zaitsev (HERA-B Collaboration), Phys. At. Nucl. **72**, 675 (2009).
- [21] V. Khachatryan et al. (CMS Collaboration), Phys. Rev. Lett. **106**, 112001 (2011).
- [22] S. Chatrchyan et al. (CMS Collaboration), Phys. Rev. Lett. **106**, 252001 (2011).
- [23] S. Chatrchyan et al. (CMS Collaboration), Phys. Rev. **D84**, 052008 (2011).
- [24] R. Aaij et al. (LHCb Collaboration), Phys. Lett. **B 694**, 209 (2010).
- [25] V. Khachatryan et al. (CMS Collaboration), J. High Energy Phys. **03**, 090 (2011).
- [26] K. Aamodt et al. (ALICE Collaboration), JINST **3**, S08002 (2008).
- [27] K. Aamodt et al. (ALICE Collaboration), JINST **5**, P03003 (2010).
- [28] J. Alme et al. (ALICE Collaboration), Nucl. Inst. Meth. **A622**, 316 (2010).
- [29] B. Abelev et al. (ALICE Collaboration), J. High Energy Phys. **1**, 128 (2012).
- [30] K. Nakamura et al. (Particle Data Group), J. Phys. **G37**, 075021 (2010).
- [31] J.E. Gaiser, Ph.D. Thesis (pag.178), SLAC-R-255 (1982).
- [32] R. Brun et al., CERN Program Library Long Write-up, W5013, GEANT Detector Description and Simulation Tool (1994).
- [33] D. Stocco et al., ALICE Internal Note ALICE-INT-2006-029, <https://edms.cern.ch/document/803009/1>.
- [34] T. Sjöstrand, Comput. Phys. Commun. **82**, 74 (1994).



- [35] T. Sjöstrand, S. Mrenna and P. Skands, JHEP **05**, 026 (2006).
- [36] P.Z. Skands, arXiv:1005.3457 (2010).
- [37] D.J. Lange, Nucl. Instrum. Meth. A **462**, 152 (2001).
- [38] E. Barberio, B. van Eijk and Z. Was, Comput. Phys. Commun. **66**, 115 (1991).
- [39] E. Barberio and Z. Was, Comput. Phys. Commun. **79**, 291 (1994).
- [40] B. Aubert et al. (BaBar Collaboration), Phys. Rev. D **67**, 032002 (2003).
- [41] M. Cacciari, S. Frixione, M.L. Mangano, P. Nason, and G. Ridolfi, J. High Energy Phys. **07**, 033 (2004).
- [42] M. Cacciari, S. Frixione, N. Houdeau, M.L. Mangano, P. Nason and G. Ridolfi, arXiv:1205.6344 (2012).
- [43] P.M. Nadolsky et al., Phys. Rev. D **78**, 013004 (2008).
- [44] P. Abreu et al. (DELPHI Collaboration), Phys. Lett. B **341**, 109 (1994).
- [45] O. Adriani et al. (L3 Collaboration), Phys. Lett. B **317**, 467 (1993).
- [46] D. Buskulic et al. (ALEPH Collaboration), Phys. Lett. B **295**, 396 (1992).
- [47] A. Adare et al. (PHENIX Collaboration), Phys. Rev. Lett. **103**, 082002 (2009).

## 6 Acknowledgements

The ALICE collaboration would like to thank all its engineers and technicians for their invaluable contributions to the construction of the experiment and the CERN accelerator teams for the outstanding performance of the LHC complex.

The ALICE collaboration would like to thank M. Butenschön and B.A. Kniehl, Y.-Q. Ma, K. Wang and K.T. Chao, and V.A. Saleev, M.A. Nefedov and A.V. Shipilova for providing their theoretical computations of the production cross section of prompt  $J/\psi$ , and M. Cacciari for predictions in the FONLL scheme.

The ALICE collaboration acknowledges the following funding agencies for their support in building and running the ALICE detector:

Calouste Gulbenkian Foundation from Lisbon and Swiss Fonds Kidagan, Armenia;

Conselho Nacional de Desenvolvimento Científico e Tecnológico (CNPq), Financiadora de Estudos e Projetos (FINEP), Fundação de Amparo à Pesquisa do Estado de São Paulo (FAPESP);

National Natural Science Foundation of China (NSFC), the Chinese Ministry of Education (CMOE) and the Ministry of Science and Technology of China (MSTC);

Ministry of Education and Youth of the Czech Republic;

Danish Natural Science Research Council, the Carlsberg Foundation and the Danish National Research Foundation;

The European Research Council under the European Community's Seventh Framework Programme;

Helsinki Institute of Physics and the Academy of Finland;

French CNRS-IN2P3, the 'Region Pays de Loire', 'Region Alsace', 'Region Auvergne' and CEA, France;

German BMBF and the Helmholtz Association;

General Secretariat for Research and Technology, Ministry of Development, Greece;

Hungarian OTKA and National Office for Research and Technology (NKTH);

Department of Atomic Energy and Department of Science and Technology of the Government of India;

Istituto Nazionale di Fisica Nucleare (INFN) of Italy;

MEXT Grant-in-Aid for Specially Promoted Research, Japan;

Joint Institute for Nuclear Research, Dubna;

National Research Foundation of Korea (NRF);

CONACYT, DGAPA, México, ALFA-EC and the HELEN Program (High-Energy physics Latin-American–

European Network);

Stichting voor Fundamenteel Onderzoek der Materie (FOM) and the Nederlandse Organisatie voor Wetenschappelijk Onderzoek (NWO), Netherlands;

Research Council of Norway (NFR);

Polish Ministry of Science and Higher Education;

National Authority for Scientific Research - NASR (Autoritatea Națională pentru Cercetare Științifică - ANCS);

Federal Agency of Science of the Ministry of Education and Science of Russian Federation, International Science and Technology Center, Russian Academy of Sciences, Russian Federal Agency of Atomic Energy, Russian Federal Agency for Science and Innovations and CERN-INTAS;

Ministry of Education of Slovakia;

Department of Science and Technology, South Africa;

CIEMAT, EELA, Ministerio de Educación y Ciencia of Spain, Xunta de Galicia (Consellería de Educación), CEADEN, Cubaenergía, Cuba, and IAEA (International Atomic Energy Agency);

Swedish Research Council (VR) and Knut & Alice Wallenberg Foundation (KAW);

Ukraine Ministry of Education and Science;

United Kingdom Science and Technology Facilities Council (STFC);

The United States Department of Energy, the United States National Science Foundation, the State of Texas, and the State of Ohio.

## A The ALICE Collaboration

B. Abelev<sup>68</sup>, J. Adam<sup>33</sup>, D. Adamová<sup>73</sup>, A.M. Adare<sup>120</sup>, M.M. Aggarwal<sup>77</sup>, G. Aglieri Rinella<sup>29</sup>, A.G. Agocs<sup>60</sup>, A. Agostinelli<sup>21</sup>, S. Aguilar Salazar<sup>56</sup>, Z. Ahammed<sup>116</sup>, A. Ahmad Masoodi<sup>13</sup>, N. Ahmad<sup>13</sup>, S.A. Ahn<sup>62</sup>, S.U. Ahn<sup>63,36</sup>, A. Akindinov<sup>46</sup>, D. Aleksandrov<sup>88</sup>, B. Alessandro<sup>94</sup>, R. Alfaro Molina<sup>56</sup>, A. Alici<sup>97,9</sup>, A. Alkin<sup>2</sup>, E. Almaráz Aviña<sup>56</sup>, J. Alme<sup>31</sup>, T. Alt<sup>35</sup>, V. Altini<sup>27</sup>, S. Altinpinar<sup>14</sup>, I. Altsybeev<sup>117</sup>, C. Andrei<sup>70</sup>, A. Andronic<sup>85</sup>, V. Anguelov<sup>82</sup>, J. Anielski<sup>54</sup>, C. Anson<sup>15</sup>, T. Antičić<sup>86</sup>, F. Antinori<sup>93</sup>, P. Antonioli<sup>97</sup>, L. Aphecetche<sup>102</sup>, H. Appelshäuser<sup>52</sup>, N. Arbor<sup>64</sup>, S. Arce<sup>21</sup>, A. Arend<sup>52</sup>, N. Armesto<sup>12</sup>, R. Arnaldi<sup>94</sup>, T. Aronsson<sup>120</sup>, I.C. Arsene<sup>85</sup>, M. Arslanok<sup>52</sup>, A. Asryan<sup>117</sup>, A. Augustinus<sup>29</sup>, R. Averbeck<sup>85</sup>, T.C. Awes<sup>74</sup>, J. Äystö<sup>37</sup>, M.D. Azmi<sup>13</sup>, M. Bach<sup>35</sup>, A. Badalà<sup>99</sup>, Y.W. Baek<sup>63,36</sup>, R. Bailhache<sup>52</sup>, R. Bala<sup>94</sup>, R. Baldini Ferroli<sup>9</sup>, A. Baldisseri<sup>11</sup>, A. Baldit<sup>63</sup>, F. Baltasar Dos Santos Pedrosa<sup>29</sup>, J. Bán<sup>47</sup>, R.C. Baral<sup>48</sup>, R. Barbera<sup>23</sup>, F. Barile<sup>27</sup>, G.G. Barnaföldi<sup>60</sup>, L.S. Barnby<sup>90</sup>, V. Barret<sup>63</sup>, J. Bartke<sup>104</sup>, M. Basile<sup>21</sup>, N. Bastid<sup>63</sup>, S. Basu<sup>116</sup>, B. Bathen<sup>54</sup>, G. Batigne<sup>102</sup>, B. Batyunya<sup>59</sup>, C. Baumann<sup>52</sup>, I.G. Bearden<sup>71</sup>, H. Beck<sup>52</sup>, I. Belikov<sup>58</sup>, F. Bellini<sup>21</sup>, R. Bellwied<sup>110</sup>, E. Belmont-Moreno<sup>56</sup>, G. Bencedi<sup>60</sup>, S. Beole<sup>25</sup>, I. Berceanu<sup>70</sup>, A. Bercuci<sup>70</sup>, Y. Berdnikov<sup>75</sup>, D. Berenyi<sup>60</sup>, A.A.E. Bergognon<sup>102</sup>, D. Berzano<sup>94</sup>, L. Betev<sup>29</sup>, A. Bhasin<sup>80</sup>, A.K. Bhati<sup>77</sup>, J. Bhom<sup>114</sup>, L. Bianchi<sup>25</sup>, N. Bianchi<sup>65</sup>, C. Bianchin<sup>19</sup>, J. Bielčák<sup>33</sup>, J. Bielčíková<sup>73</sup>, A. Bilandzic<sup>72,71</sup>, S. Bjelogrić<sup>45</sup>, F. Blanco<sup>7</sup>, F. Blanco<sup>110</sup>, D. Blau<sup>88</sup>, C. Blume<sup>52</sup>, M. Boccioni<sup>29</sup>, N. Bock<sup>15</sup>, S. Böttger<sup>51</sup>, A. Bogdanov<sup>69</sup>, H. Bøggild<sup>71</sup>, M. Bogolyubsky<sup>43</sup>, L. Boldizsár<sup>60</sup>, M. Bombara<sup>34</sup>, J. Book<sup>52</sup>, H. Borel<sup>11</sup>, A. Borissov<sup>119</sup>, S. Bose<sup>89</sup>, F. Bossú<sup>25</sup>, M. Botje<sup>72</sup>, B. Boyer<sup>42</sup>, E. Braidot<sup>67</sup>, P. Braun-Munzinger<sup>85</sup>, M. Bregant<sup>102</sup>, T. Breitner<sup>51</sup>, T.A. Browning<sup>83</sup>, M. Broz<sup>32</sup>, R. Brun<sup>29</sup>, E. Bruna<sup>25,94</sup>, G.E. Bruno<sup>27</sup>, D. Budnikov<sup>87</sup>, H. Buesching<sup>52</sup>, S. Bufalino<sup>25,94</sup>, K. Bugaiev<sup>2</sup>, O. Busch<sup>82</sup>, Z. Buthelezi<sup>79</sup>, D. Caballero Orduna<sup>120</sup>, D. Caffarri<sup>19</sup>, X. Cai<sup>39</sup>, H. Caines<sup>120</sup>, E. Calvo Villar<sup>91</sup>, P. Camerini<sup>20</sup>, V. Canoa Roman<sup>8,1</sup>, G. Cara Romeo<sup>97</sup>, F. Carena<sup>29</sup>, W. Carena<sup>29</sup>, N. Carlin Filho<sup>107</sup>, F. Carminati<sup>29</sup>, C.A. Carrillo Montoya<sup>29</sup>, A. Casanova Díaz<sup>65</sup>, J. Castillo Castellanos<sup>11</sup>, J.F. Castillo Hernandez<sup>85</sup>, E.A.R. Casula<sup>18</sup>, V. Catanescu<sup>70</sup>, C. Cavicchioli<sup>29</sup>, C. Ceballos Sanchez<sup>6</sup>, J. Cepila<sup>33</sup>, P. Cerello<sup>94</sup>, B. Chang<sup>37,123</sup>, S. Chapeland<sup>29</sup>, J.L. Charvet<sup>11</sup>, S. Chattopadhyay<sup>116</sup>, S. Chattopadhyay<sup>89</sup>, I. Chawla<sup>77</sup>, M. Cherney<sup>76</sup>, C. Cheshkov<sup>29,109</sup>, B. Cheynis<sup>109</sup>, V. Chibante Barroso<sup>29</sup>, D.D. Chinellato<sup>108</sup>, P. Chochula<sup>29</sup>, M. Chojnacki<sup>45</sup>, S. Choudhury<sup>116</sup>, P. Christakoglou<sup>72,45</sup>, C.H. Christensen<sup>71</sup>, P. Christiansen<sup>28</sup>, T. Chujo<sup>114</sup>, S.U. Chung<sup>84</sup>, C. Cicalo<sup>96</sup>, L. Cifarelli<sup>21,29,9</sup>, F. Cindolo<sup>97</sup>, J. Cleymans<sup>79</sup>, F. Coccetti<sup>9</sup>, F. Colamaria<sup>27</sup>, D. Colella<sup>27</sup>, G. Conesa Balbastre<sup>64</sup>, Z. Conesa del Valle<sup>29</sup>, P. Constantin<sup>82</sup>, G. Contin<sup>20</sup>, J.G. Contreras<sup>8</sup>, T.M. Cormier<sup>119</sup>, Y. Corrales Morales<sup>25</sup>, P. Cortese<sup>26</sup>, I. Cortés Maldonado<sup>1</sup>, M.R. Cosentino<sup>67</sup>, F. Costa<sup>29</sup>, M.E. Cotallo<sup>7</sup>, E. Crescio<sup>8</sup>, P. Crochet<sup>63</sup>, E. Cruz Alaniz<sup>56</sup>, E. Cuautle<sup>55</sup>, L. Cunqueiro<sup>65</sup>, A. Dainese<sup>19,93</sup>, H.H. Dalsgaard<sup>71</sup>, A. Danu<sup>50</sup>, D. Das<sup>89</sup>, I. Das<sup>42</sup>, K. Das<sup>89</sup>, S. Dash<sup>40</sup>, A. Dash<sup>108</sup>, S. De<sup>116</sup>, G.O.V. de Barros<sup>107</sup>, A. De Caro<sup>24,9</sup>, G. de Cataldo<sup>98</sup>, J. de Cuveland<sup>35</sup>, A. De Falco<sup>18</sup>, D. De Gruttola<sup>24</sup>, H. Delagrèze<sup>102</sup>, A. Deloff<sup>100</sup>, V. Demanov<sup>87</sup>, N. De Marco<sup>94</sup>, E. Dénes<sup>60</sup>, S. De Pasquale<sup>24</sup>, A. Deppman<sup>107</sup>, G. D'Erasmus<sup>27</sup>, R. de Rooij<sup>45</sup>, M.A. Diaz Corchero<sup>7</sup>, D. Di Bari<sup>27</sup>, C. Di Giglio<sup>27</sup>, T. Dietel<sup>54</sup>, S. Di Liberto<sup>95</sup>, A. Di Mauro<sup>29</sup>, P. Di Nezza<sup>65</sup>, R. Divià<sup>29</sup>, Ø. Djuvsland<sup>14</sup>, A. Dobrin<sup>119,28</sup>, T. Dobrowolski<sup>100</sup>, I. Domínguez<sup>55</sup>, B. Dönigus<sup>85</sup>, O. Dordic<sup>17</sup>, O. Driga<sup>102</sup>, A.K. Dubey<sup>116</sup>, L. Ducroux<sup>109</sup>, P. Dupieux<sup>63</sup>, M.R. Dutta Majumdar<sup>116</sup>, A.K. Dutta Majumdar<sup>89</sup>, D. Elia<sup>98</sup>, D. Emschermann<sup>54</sup>, H. Engel<sup>51</sup>, H.A. Erdal<sup>31</sup>, B. Espagnon<sup>42</sup>, M. Estienne<sup>102</sup>, S. Esumi<sup>114</sup>, D. Evans<sup>90</sup>, G. Eyyubova<sup>17</sup>, D. Fabris<sup>19,93</sup>, J. Faivre<sup>64</sup>, D. Falchieri<sup>21</sup>, A. Fantoni<sup>65</sup>, M. Fasel<sup>85</sup>, R. Fearick<sup>79</sup>, A. Fedunov<sup>59</sup>, D. Fehlinger<sup>14</sup>, L. Feldkamp<sup>54</sup>, D. Felea<sup>50</sup>, B. Fenton-Olsen<sup>67</sup>, G. Feofilov<sup>117</sup>, A. Fernández Téllez<sup>1</sup>, A. Ferretti<sup>25</sup>, R. Ferretti<sup>26</sup>, J. Figiel<sup>104</sup>, M.A.S. Figueredo<sup>107</sup>, S. Filchagin<sup>87</sup>, D. Finogeev<sup>44</sup>, F.M. Fionda<sup>27</sup>, E.M. Fiore<sup>27</sup>, M. Floris<sup>29</sup>, S. Foertsch<sup>79</sup>, P. Foka<sup>85</sup>, S. Fokin<sup>88</sup>, E. Fragiaco<sup>92</sup>, U. Frankfeld<sup>85</sup>, U. Fuchs<sup>29</sup>, C. Furget<sup>64</sup>, M. Fusco Girard<sup>24</sup>, J.J. Gaardhøje<sup>71</sup>, M. Gagliardi<sup>25</sup>, A. Gago<sup>91</sup>, M. Gallio<sup>25</sup>, D.R. Gangadharan<sup>15</sup>, P. Ganoti<sup>74</sup>, C. Garabatos<sup>85</sup>, E. Garcia-Solis<sup>10</sup>, I. Garishvili<sup>68</sup>, J. Gerhard<sup>35</sup>, M. Germain<sup>102</sup>, C. Geuna<sup>11</sup>, A. Gheata<sup>29</sup>, M. Gheata<sup>50,29</sup>, B. Ghidini<sup>27</sup>, P. Ghosh<sup>116</sup>, P. Gianotti<sup>65</sup>, M.R. Girard<sup>118</sup>, P. Giubellino<sup>29</sup>, E. Gladysz-Dziadus<sup>104</sup>, P. Glässel<sup>82</sup>, R. Gomez<sup>106</sup>, A. Gonschior<sup>85</sup>, E.G. Ferreira<sup>12</sup>, L.H. González-Trueba<sup>56</sup>, P. González-Zamora<sup>7</sup>, S. Gorbunov<sup>35</sup>, A. Goswami<sup>81</sup>, S. Gotovac<sup>103</sup>, V. Grabski<sup>56</sup>, L.K. Graczykowski<sup>118</sup>, R. Grajcarek<sup>82</sup>, A. Grelli<sup>45</sup>, C. Grigoras<sup>29</sup>, A. Grigoras<sup>29</sup>, V. Grigoriev<sup>69</sup>, A. Grigoryan<sup>121</sup>, S. Grigoryan<sup>59</sup>, B. Grinyov<sup>2</sup>, N. Grion<sup>92</sup>, P. Gros<sup>28</sup>, J.F. Grosse-Oetringhaus<sup>29</sup>, J.-Y. Grossiord<sup>109</sup>, R. Grosso<sup>29</sup>, F. Guber<sup>44</sup>, R. Guernane<sup>64</sup>, C. Guerra Gutierrez<sup>91</sup>, B. Guerzoni<sup>21</sup>, M. Guilbaud<sup>109</sup>, K. Gulbrandsen<sup>71</sup>, T. Gunji<sup>113</sup>, A. Gupta<sup>80</sup>, R. Gupta<sup>80</sup>, H. Gutbrod<sup>85</sup>, Ø. Haaland<sup>14</sup>, C. Hadjidakis<sup>42</sup>, M. Haiduc<sup>50</sup>, H. Hamagaki<sup>113</sup>, G. Hamar<sup>60</sup>, B.H. Han<sup>16</sup>, L.D. Hanratty<sup>90</sup>, A. Hansen<sup>71</sup>, Z. Harmanova<sup>34</sup>, J.W. Harris<sup>120</sup>, M. Hartig<sup>52</sup>, D. Hasegan<sup>50</sup>, D. Hatzifotiadou<sup>97</sup>, A. Hayrapetyan<sup>29,121</sup>, S.T. Heckel<sup>52</sup>, M. Heide<sup>54</sup>, H. Helstrup<sup>31</sup>, A. Herghelegiu<sup>70</sup>, G. Herrera Corral<sup>8</sup>, N. Herrmann<sup>82</sup>, B.A. Hess<sup>115</sup>, K.F. Hetland<sup>31</sup>, B. Hicks<sup>120</sup>, P.T. Hille<sup>120</sup>, B. Hippolyte<sup>58</sup>, T. Horaguchi<sup>114</sup>, Y. Hori<sup>113</sup>, P. Hristov<sup>29</sup>, I. Hřivnáčová<sup>42</sup>, M. Huang<sup>14</sup>, T.J. Humanic<sup>15</sup>, D.S. Hwang<sup>16</sup>, R. Ichou<sup>63</sup>, R. Ilkaev<sup>87</sup>,

I. Ilkiv<sup>100</sup>, M. Inaba<sup>114</sup>, E. Incani<sup>18</sup>, G.M. Innocenti<sup>25</sup>, P.G. Innocenti<sup>29</sup>, M. Ippolitov<sup>88</sup>, M. Irfan<sup>13</sup>, C. Ivan<sup>85</sup>, V. Ivanov<sup>75</sup>, M. Ivanov<sup>85</sup>, A. Ivanov<sup>117</sup>, O. Ivanytskyi<sup>2</sup>, A. Jachořkowski<sup>29</sup>, P. M. Jacobs<sup>67</sup>, H.J. Jang<sup>62</sup>, S. Jangal<sup>58</sup>, M.A. Janik<sup>118</sup>, R. Janik<sup>32</sup>, P.H.S.Y. Jayarathna<sup>110</sup>, S. Jena<sup>40</sup>, D.M. Jha<sup>119</sup>, R.T. Jimenez Bustamante<sup>55</sup>, L. Jiriden<sup>29</sup>, P.G. Jones<sup>90</sup>, H. Jung<sup>36</sup>, A. Jusko<sup>90</sup>, A.B. Kaidalov<sup>46</sup>, V. Kakoyan<sup>121</sup>, S. Kalcher<sup>35</sup>, P. Kaliňák<sup>47</sup>, T. Kalliokoski<sup>37</sup>, A. Kalweit<sup>53</sup>, K. Kanaki<sup>14</sup>, J.H. Kang<sup>123</sup>, V. Kaplin<sup>69</sup>, A. Karasu Uysal<sup>29,122</sup>, O. Karavichev<sup>44</sup>, T. Karavicheva<sup>44</sup>, E. Karpechev<sup>44</sup>, A. Kazantsev<sup>88</sup>, U. Kebschull<sup>51</sup>, R. Keidel<sup>124</sup>, P. Khan<sup>89</sup>, M.M. Khan<sup>13</sup>, S.A. Khan<sup>116</sup>, A. Khanzadeev<sup>75</sup>, Y. Kharlov<sup>43</sup>, B. Kileng<sup>31</sup>, D.W. Kim<sup>36</sup>, M.Kim<sup>36</sup>, M. Kim<sup>123</sup>, S.H. Kim<sup>36</sup>, D.J. Kim<sup>37</sup>, S. Kim<sup>16</sup>, J.H. Kim<sup>16</sup>, J.S. Kim<sup>36</sup>, B. Kim<sup>123</sup>, T. Kim<sup>123</sup>, S. Kirsch<sup>35</sup>, I. Kisel<sup>35</sup>, S. Kiselev<sup>46</sup>, A. Kisiel<sup>29,118</sup>, J.L. Klay<sup>4</sup>, J. Klein<sup>82</sup>, C. Klein-Bösing<sup>54</sup>, M. Kliemant<sup>52</sup>, A. Kluge<sup>29</sup>, M.L. Knichel<sup>85</sup>, A.G. Knospe<sup>105</sup>, K. Koch<sup>82</sup>, M.K. Köhler<sup>85</sup>, A. Kolojvari<sup>117</sup>, V. Kondratiev<sup>117</sup>, N. Kondratyeva<sup>69</sup>, A. Konevskikh<sup>44</sup>, A. Korneev<sup>87</sup>, R. Kour<sup>90</sup>, M. Kowalski<sup>104</sup>, S. Kox<sup>64</sup>, G. Koyithatta Meethalevedu<sup>40</sup>, J. Kral<sup>37</sup>, I. Králík<sup>47</sup>, F. Kramer<sup>52</sup>, I. Kraus<sup>85</sup>, T. Krawutschke<sup>82,30</sup>, M. Krelina<sup>33</sup>, M. Kretz<sup>35</sup>, M. Krivda<sup>90,47</sup>, F. Krizek<sup>37</sup>, M. Krus<sup>33</sup>, E. Kryshen<sup>75</sup>, M. Krzewicki<sup>85</sup>, Y. Kucheriaev<sup>88</sup>, C. Kuhn<sup>58</sup>, P.G. Kuijter<sup>72</sup>, I. Kulakov<sup>52</sup>, J. Kumar<sup>40</sup>, P. Kurashvili<sup>100</sup>, A.B. Kurepin<sup>44</sup>, A. Kurepin<sup>44</sup>, A. Kuryakin<sup>87</sup>, V. Kuschpil<sup>73</sup>, S. Kuschpil<sup>73</sup>, H. Kvaerno<sup>17</sup>, M.J. Kweon<sup>82</sup>, Y. Kwon<sup>123</sup>, P. Ladrón de Guevara<sup>55</sup>, I. Lakomov<sup>42</sup>, R. Langoy<sup>14</sup>, S.L. La Pointe<sup>45</sup>, C. Lara<sup>51</sup>, A. Lardeux<sup>102</sup>, P. La Rocca<sup>23</sup>, C. Lazzeroni<sup>90</sup>, R. Lea<sup>20</sup>, Y. Le Bornec<sup>42</sup>, M. Lechman<sup>29</sup>, S.C. Lee<sup>36</sup>, K.S. Lee<sup>36</sup>, G.R. Lee<sup>90</sup>, F. Lefèvre<sup>102</sup>, J. Lehnert<sup>52</sup>, L. Leistam<sup>29</sup>, M. Lenhardt<sup>102</sup>, V. Lenti<sup>98</sup>, H. León<sup>56</sup>, M. Leoncino<sup>94</sup>, I. León Monzón<sup>106</sup>, H. León Vargas<sup>52</sup>, P. Lévai<sup>60</sup>, J. Lien<sup>14</sup>, R. Lietava<sup>90</sup>, S. Lindal<sup>17</sup>, V. Lindenstruth<sup>35</sup>, C. Lippmann<sup>85,29</sup>, M.A. Lisa<sup>15</sup>, L. Liu<sup>14</sup>, P.I. Loenne<sup>14</sup>, V.R. Loggins<sup>119</sup>, V. Loginov<sup>69</sup>, S. Lohn<sup>29</sup>, D. Lohner<sup>82</sup>, C. Loizides<sup>67</sup>, K.K. Loo<sup>37</sup>, X. Lopez<sup>63</sup>, E. López Torres<sup>6</sup>, G. Løvnhøiden<sup>17</sup>, X.-G. Lu<sup>82</sup>, P. Luettig<sup>52</sup>, M. Lunardon<sup>19</sup>, J. Luo<sup>39</sup>, G. Luparello<sup>45</sup>, L. Luquin<sup>102</sup>, C. Luzzi<sup>29</sup>, R. Ma<sup>120</sup>, K. Ma<sup>39</sup>, D.M. Madagodahettige-Don<sup>110</sup>, A. Maevskaya<sup>44</sup>, M. Mager<sup>53,29</sup>, D.P. Mahapatra<sup>48</sup>, A. Maire<sup>82</sup>, M. Malaev<sup>75</sup>, I. Maldonado Cervantes<sup>55</sup>, L. Malinina<sup>59,i</sup>, D. Mal'Kevich<sup>46</sup>, P. Malzacher<sup>85</sup>, A. Mamonov<sup>87</sup>, L. Manceau<sup>94</sup>, L. Mangotra<sup>80</sup>, V. Manko<sup>88</sup>, F. Manso<sup>63</sup>, V. Manzari<sup>98</sup>, Y. Mao<sup>39</sup>, M. Marchisone<sup>63,25</sup>, J. Mareš<sup>49</sup>, G.V. Margagliotti<sup>20,92</sup>, A. Margotti<sup>97</sup>, A. Marín<sup>85</sup>, C.A. Marin Tobon<sup>29</sup>, C. Markert<sup>105</sup>, I. Martashvili<sup>112</sup>, P. Martinengo<sup>29</sup>, M.I. Martínez<sup>1</sup>, A. Martínez Davalos<sup>56</sup>, G. Martínez García<sup>102</sup>, Y. Martynov<sup>2</sup>, A. Mas<sup>102</sup>, S. Masciocchi<sup>85</sup>, M. Maserà<sup>25</sup>, A. Masoni<sup>96</sup>, L. Massacrier<sup>109,102</sup>, M. Mastromarco<sup>98</sup>, A. Mastroserio<sup>27,29</sup>, Z.L. Matthews<sup>90</sup>, A. Matyja<sup>104,102</sup>, D. Mayani<sup>55</sup>, C. Mayer<sup>104</sup>, J. Mazer<sup>112</sup>, M.A. Mazzoni<sup>95</sup>, F. Meddi<sup>22</sup>, A. Menchaca-Rocha<sup>56</sup>, J. Mercado Pérez<sup>82</sup>, M. Meres<sup>32</sup>, Y. Miake<sup>114</sup>, L. Milano<sup>25</sup>, J. Milosevic<sup>17,ii</sup>, A. Mischke<sup>45</sup>, A.N. Mishra<sup>81</sup>, D. Miśkowiec<sup>85,29</sup>, C. Mitu<sup>50</sup>, J. Mlynarz<sup>119</sup>, B. Mohanty<sup>116</sup>, A.K. Mohanty<sup>29</sup>, L. Molnar<sup>29</sup>, L. Montaño Zetina<sup>8</sup>, M. Monteno<sup>94</sup>, E. Montes<sup>7</sup>, T. Moon<sup>123</sup>, M. Morando<sup>19</sup>, D.A. Moreira De Godoy<sup>107</sup>, S. Moretto<sup>19</sup>, A. Morsch<sup>29</sup>, V. Muccifora<sup>65</sup>, E. Mudnic<sup>103</sup>, S. Muhuri<sup>116</sup>, M. Mukherjee<sup>116</sup>, H. Müller<sup>29</sup>, M.G. Munhoz<sup>107</sup>, L. Musa<sup>29</sup>, A. Musso<sup>94</sup>, B.K. Nandi<sup>40</sup>, R. Nania<sup>97</sup>, E. Nappi<sup>98</sup>, C. Nattrass<sup>112</sup>, N.P. Naumov<sup>87</sup>, S. Navin<sup>90</sup>, T.K. Nayak<sup>116</sup>, S. Nazarenko<sup>87</sup>, G. Nazarov<sup>87</sup>, A. Nedosekin<sup>46</sup>, M. Nicassio<sup>27</sup>, M. Niculescu<sup>50,29</sup>, B.S. Nielsen<sup>71</sup>, T. Niida<sup>114</sup>, S. Nikolaev<sup>88</sup>, V. Nikolic<sup>86</sup>, S. Nikulin<sup>88</sup>, V. Nikulin<sup>75</sup>, B.S. Nilsen<sup>76</sup>, M.S. Nilsson<sup>17</sup>, F. Noferini<sup>97,9</sup>, P. Nomokonov<sup>59</sup>, G. Nooren<sup>45</sup>, N. Novitzky<sup>37</sup>, A. Nyanin<sup>88</sup>, A. Nyatha<sup>40</sup>, C. Nygaard<sup>71</sup>, J. Nystrand<sup>14</sup>, A. Ochirov<sup>117</sup>, H. Oeschler<sup>53,29</sup>, S. Oh<sup>120</sup>, S.K. Oh<sup>36</sup>, J. Oleniacz<sup>118</sup>, C. Oppedisano<sup>94</sup>, A. Ortiz Velasquez<sup>28,55</sup>, G. Ortona<sup>25</sup>, A. Oskarsson<sup>28</sup>, P. Ostrowski<sup>118</sup>, J. Otwinowski<sup>85</sup>, K. Oyama<sup>82</sup>, K. Ozawa<sup>113</sup>, Y. Pachmayer<sup>82</sup>, M. Pachr<sup>33</sup>, F. Padilla<sup>25</sup>, P. Pagano<sup>24</sup>, G. Paić<sup>55</sup>, F. Painke<sup>35</sup>, C. Pajares<sup>12</sup>, S. Pal<sup>11</sup>, S.K. Pal<sup>116</sup>, A. Palaha<sup>90</sup>, A. Palmeri<sup>99</sup>, V. Papikyan<sup>121</sup>, G.S. Pappalardo<sup>99</sup>, W.J. Park<sup>85</sup>, A. Passfeld<sup>54</sup>, B. Pastirčák<sup>47</sup>, D.I. Patalakha<sup>43</sup>, V. Paticchio<sup>98</sup>, A. Pavlinov<sup>119</sup>, T. Pawlak<sup>118</sup>, T. Peitzmann<sup>45</sup>, H. Pereira Da Costa<sup>11</sup>, E. Pereira De Oliveira Filho<sup>107</sup>, D. Peresunko<sup>88</sup>, C.E. Pérez Lara<sup>72</sup>, E. Perez Lezama<sup>55</sup>, D. Perini<sup>29</sup>, D. Perrino<sup>27</sup>, W. Peryt<sup>118</sup>, A. Pesci<sup>97</sup>, V. Peskov<sup>29,55</sup>, Y. Pestov<sup>3</sup>, V. Petráček<sup>33</sup>, M. Petran<sup>33</sup>, M. Petris<sup>70</sup>, P. Petrov<sup>90</sup>, M. Petrovici<sup>70</sup>, C. Petta<sup>23</sup>, S. Piano<sup>92</sup>, A. Piccotti<sup>94</sup>, M. Pikna<sup>32</sup>, P. Pillot<sup>102</sup>, O. Pinazza<sup>29</sup>, L. Pinsky<sup>110</sup>, N. Pitz<sup>52</sup>, D.B. Piyarathna<sup>110</sup>, M. Płoskoń<sup>67</sup>, J. Pluta<sup>118</sup>, T. Pocheptsov<sup>59</sup>, S. Pochybova<sup>60</sup>, P.L.M. Podesta-Lerma<sup>106</sup>, M.G. Poghosyan<sup>29,25</sup>, K. Polák<sup>49</sup>, B. Polichtchouk<sup>43</sup>, A. Pop<sup>70</sup>, S. Porteboeuf-Houssais<sup>63</sup>, V. Pospíšil<sup>33</sup>, B. Potukuchi<sup>80</sup>, S.K. Prasad<sup>119</sup>, R. Preghenella<sup>97,9</sup>, F. Prino<sup>94</sup>, C.A. Pruneau<sup>119</sup>, I. Pshenichnov<sup>44</sup>, S. Puchagin<sup>87</sup>, G. Puudu<sup>18</sup>, J. Pujol Teixido<sup>51</sup>, A. Pulvirenti<sup>23,29</sup>, V. Punin<sup>87</sup>, M. Putiš<sup>34</sup>, J. Putschke<sup>119,120</sup>, E. Quercigh<sup>29</sup>, H. Qvigstad<sup>17</sup>, A. Rachevski<sup>92</sup>, A. Rademakers<sup>29</sup>, S. Radomski<sup>82</sup>, T.S. Rähä<sup>37</sup>, J. Rak<sup>37</sup>, A. Rakotozafindrabe<sup>11</sup>, L. Ramello<sup>26</sup>, A. Ramírez Reyes<sup>8</sup>, S. Raniwala<sup>81</sup>, R. Raniwala<sup>81</sup>, S.S. Räsänen<sup>37</sup>, B.T. Rascanu<sup>52</sup>, D. Rathee<sup>77</sup>, K.F. Read<sup>112</sup>, J.S. Real<sup>64</sup>, K. Redlich<sup>100,57</sup>, P. Reichelt<sup>52</sup>, M. Reicher<sup>45</sup>, R. Renfordt<sup>52</sup>, A.R. Reolon<sup>65</sup>, A. Reshetin<sup>44</sup>, F. Rettig<sup>35</sup>, J.-P. Revol<sup>29</sup>, K. Reygers<sup>82</sup>, L. Riccati<sup>94</sup>, R.A. Ricci<sup>66</sup>, T. Richert<sup>28</sup>, M. Richter<sup>17</sup>, P. Riedler<sup>29</sup>, W. Riegler<sup>29</sup>, F. Riggi<sup>23,99</sup>, B. Rodrigues Fernandes Rabacal<sup>29</sup>, M. Rodríguez Cahuantzi<sup>1</sup>, A. Rodríguez Manso<sup>72</sup>, K. Røed<sup>14</sup>, D. Rohr<sup>35</sup>,

D. Röhrich<sup>14</sup>, R. Romita<sup>85</sup>, F. Ronchetti<sup>65</sup>, P. Rosnet<sup>63</sup>, S. Rossegger<sup>29</sup>, A. Rossi<sup>29,19</sup>, C. Roy<sup>58</sup>, P. Roy<sup>89</sup>, A.J. Rubio Montero<sup>7</sup>, R. Rui<sup>20</sup>, E. Ryabinkin<sup>88</sup>, A. Rybicki<sup>104</sup>, S. Sadovsky<sup>43</sup>, K. Šafařík<sup>29</sup>, R. Sahoo<sup>41</sup>, P.K. Sahu<sup>48</sup>, J. Saini<sup>116</sup>, H. Sakaguchi<sup>38</sup>, S. Sakai<sup>67</sup>, D. Sakata<sup>114</sup>, C.A. Salgado<sup>12</sup>, J. Salzwedel<sup>15</sup>, S. Sambyal<sup>80</sup>, V. Samsonov<sup>75</sup>, X. Sanchez Castro<sup>58</sup>, L. Šándor<sup>47</sup>, A. Sandoval<sup>56</sup>, S. Sano<sup>113</sup>, M. Sano<sup>114</sup>, R. Santo<sup>54</sup>, R. Santoro<sup>98,29,9</sup>, J. Sarkamo<sup>37</sup>, E. Scapparone<sup>97</sup>, F. Scarlassara<sup>19</sup>, R.P. Scharenberg<sup>83</sup>, C. Schiaua<sup>70</sup>, R. Schicker<sup>82</sup>, C. Schmidt<sup>85</sup>, H.R. Schmidt<sup>115</sup>, S. Schreiner<sup>29</sup>, S. Schuchmann<sup>52</sup>, J. Schukraft<sup>29</sup>, Y. Schutz<sup>29,102</sup>, K. Schwarz<sup>85</sup>, K. Schweda<sup>85,82</sup>, G. Scioli<sup>21</sup>, E. Scomparin<sup>94</sup>, R. Scott<sup>112</sup>, P.A. Scott<sup>90</sup>, G. Segato<sup>19</sup>, I. Selyuzhenkov<sup>85</sup>, S. Senyukov<sup>26,58</sup>, J. Seo<sup>84</sup>, S. Serci<sup>18</sup>, E. Serradilla<sup>7,56</sup>, A. Sevcenco<sup>50</sup>, A. Shabetai<sup>102</sup>, G. Shabratova<sup>59</sup>, R. Shahoyan<sup>29</sup>, N. Sharma<sup>77</sup>, S. Sharma<sup>80</sup>, S. Rohni<sup>80</sup>, K. Shigaki<sup>38</sup>, M. Shimomura<sup>114</sup>, K. Shtejer<sup>6</sup>, Y. Sibiriak<sup>88</sup>, M. Siciliano<sup>25</sup>, E. Sicking<sup>29</sup>, S. Siddhanta<sup>96</sup>, T. Siemiarczuk<sup>100</sup>, D. Silvermyr<sup>74</sup>, c. Silvestre<sup>64</sup>, G. Simatovic<sup>55,86</sup>, G. Simonetti<sup>29</sup>, R. Singaraju<sup>116</sup>, R. Singh<sup>80</sup>, S. Singha<sup>116</sup>, V. Singhal<sup>116</sup>, T. Sinha<sup>89</sup>, B.C. Sinha<sup>116</sup>, B. Sitar<sup>32</sup>, M. Sitta<sup>26</sup>, T.B. Skaali<sup>17</sup>, K. Skjerdal<sup>14</sup>, R. Smakal<sup>33</sup>, N. Smirnov<sup>120</sup>, R.J.M. Snellings<sup>45</sup>, C. Sogaard<sup>71</sup>, R. Soltz<sup>68</sup>, H. Son<sup>16</sup>, M. Song<sup>123</sup>, J. Song<sup>84</sup>, C. Soos<sup>29</sup>, F. Soramel<sup>19</sup>, I. Sputowska<sup>104</sup>, M. Spyropoulou-Stassinaki<sup>78</sup>, B.K. Srivastava<sup>83</sup>, J. Stachel<sup>82</sup>, I. Stan<sup>50</sup>, I. Stan<sup>50</sup>, G. Stefanek<sup>100</sup>, T. Steinbeck<sup>35</sup>, M. Steinpreis<sup>15</sup>, E. Stenlund<sup>28</sup>, G. Steyn<sup>79</sup>, J.H. Stiller<sup>82</sup>, D. Stocco<sup>102</sup>, M. Stolpovskiy<sup>43</sup>, K. Strabykin<sup>87</sup>, P. Strmen<sup>32</sup>, A.A.P. Suaide<sup>107</sup>, M.A. Subieta Vásquez<sup>25</sup>, T. Sugitate<sup>38</sup>, C. Suire<sup>42</sup>, M. Sukhorukov<sup>87</sup>, R. Sultanov<sup>46</sup>, M. Šumbera<sup>73</sup>, T. Susa<sup>86</sup>, A. Szanto de Toledo<sup>107</sup>, I. Szarka<sup>32</sup>, A. Szczepankiewicz<sup>104</sup>, A. Szostak<sup>14</sup>, M. Szymanski<sup>118</sup>, J. Takahashi<sup>108</sup>, J.D. Tapia Takaki<sup>42</sup>, A. Tauro<sup>29</sup>, G. Tejeda Muñoz<sup>1</sup>, A. Telesca<sup>29</sup>, C. Terrevoli<sup>27</sup>, J. Thäder<sup>85</sup>, D. Thomas<sup>45</sup>, R. Tieulent<sup>109</sup>, A.R. Timmins<sup>110</sup>, D. Tlusty<sup>33</sup>, A. Toia<sup>35,29</sup>, H. Torii<sup>113</sup>, L. Toscano<sup>94</sup>, D. Truesdale<sup>15</sup>, W.H. Trzaska<sup>37</sup>, T. Tsuji<sup>113</sup>, A. Tumkin<sup>87</sup>, R. Turrisi<sup>93</sup>, T.S. Tveter<sup>17</sup>, J. Ulery<sup>52</sup>, K. Ullaland<sup>14</sup>, J. Ulrich<sup>61,51</sup>, A. Uras<sup>109</sup>, J. Urbán<sup>34</sup>, G.M. Urciuoli<sup>95</sup>, G.L. Usai<sup>18</sup>, M. Vajzer<sup>33,73</sup>, M. Vala<sup>59,47</sup>, L. Valencia Palomo<sup>42</sup>, S. Vallero<sup>82</sup>, N. van der Kolk<sup>72</sup>, P. Vande Vyvre<sup>29</sup>, M. van Leeuwen<sup>45</sup>, L. Vannucci<sup>66</sup>, A. Vargas<sup>1</sup>, R. Varma<sup>40</sup>, M. Vasileiou<sup>78</sup>, A. Vasiliev<sup>88</sup>, V. Vechernin<sup>117</sup>, M. Veldhoen<sup>45</sup>, M. Venaruzzo<sup>20</sup>, E. Vercellin<sup>25</sup>, S. Vergara<sup>1</sup>, R. Vernet<sup>5</sup>, M. Verweij<sup>45</sup>, L. Vickovic<sup>103</sup>, G. Viesti<sup>19</sup>, O. Vikhlyantsev<sup>87</sup>, Z. Vilakazi<sup>79</sup>, O. Villalobos Baillie<sup>90</sup>, A. Vinogradov<sup>88</sup>, L. Vinogradov<sup>117</sup>, Y. Vinogradov<sup>87</sup>, T. Virgili<sup>24</sup>, Y.P. Viyogi<sup>116</sup>, A. Vodopyanov<sup>59</sup>, K. Voloshin<sup>46</sup>, S. Voloshin<sup>119</sup>, G. Volpe<sup>27,29</sup>, B. von Haller<sup>29</sup>, D. Vranic<sup>85</sup>, G. Øvrebekk<sup>14</sup>, J. Vrláková<sup>34</sup>, B. Vulpescu<sup>63</sup>, A. Vyushin<sup>87</sup>, V. Wagner<sup>33</sup>, B. Wagner<sup>14</sup>, R. Wan<sup>58,39</sup>, M. Wang<sup>39</sup>, D. Wang<sup>39</sup>, Y. Wang<sup>82</sup>, Y. Wang<sup>39</sup>, K. Watanabe<sup>114</sup>, M. Weber<sup>110</sup>, J.P. Wessels<sup>29,54</sup>, U. Westerhoff<sup>54</sup>, J. Wiechula<sup>115</sup>, J. Wikne<sup>17</sup>, M. Wilde<sup>54</sup>, G. Wilk<sup>100</sup>, A. Wilk<sup>54</sup>, M.C.S. Williams<sup>97</sup>, B. Windelband<sup>82</sup>, L. Xaplanteris Karampatos<sup>105</sup>, C.G. Yaldo<sup>119</sup>, Y. Yamaguchi<sup>113</sup>, H. Yang<sup>11</sup>, S. Yang<sup>14</sup>, S. Yasnopolskiy<sup>88</sup>, J. Yi<sup>84</sup>, Z. Yin<sup>39</sup>, I.-K. Yoo<sup>84</sup>, J. Yoon<sup>123</sup>, W. Yu<sup>52</sup>, X. Yuan<sup>39</sup>, I. Yushmanov<sup>88</sup>, C. Zach<sup>33</sup>, C. Zampolli<sup>97</sup>, S. Zaporozhets<sup>59</sup>, A. Zarochentsev<sup>117</sup>, P. Závada<sup>49</sup>, N. Zaviyalov<sup>87</sup>, H. Zbroszczyk<sup>118</sup>, P. Zelnicsek<sup>51</sup>, I.S. Zgura<sup>50</sup>, M. Zhalov<sup>75</sup>, X. Zhang<sup>63,39</sup>, H. Zhang<sup>39</sup>, F. Zhou<sup>39</sup>, D. Zhou<sup>39</sup>, Y. Zhou<sup>45</sup>, J. Zhu<sup>39</sup>, J. Zhu<sup>39</sup>, X. Zhu<sup>39</sup>, A. Zichichi<sup>21,9</sup>, A. Zimmermann<sup>82</sup>, G. Zinovjev<sup>2</sup>, Y. Zoccarato<sup>109</sup>, M. Zynovyev<sup>2</sup>, M. Zyzak<sup>52</sup>

## Affiliation notes

<sup>i</sup> Also at: M.V.Lomonosov Moscow State University, D.V.Skobel'syn Institute of Nuclear Physics, Moscow, Russia

<sup>ii</sup> Also at: "Vinča" Institute of Nuclear Sciences, Belgrade, Serbia

## Collaboration Institutes

- <sup>1</sup> Benemérita Universidad Autónoma de Puebla, Puebla, Mexico
- <sup>2</sup> Bogolyubov Institute for Theoretical Physics, Kiev, Ukraine
- <sup>3</sup> Budker Institute for Nuclear Physics, Novosibirsk, Russia
- <sup>4</sup> California Polytechnic State University, San Luis Obispo, California, United States
- <sup>5</sup> Centre de Calcul de l'IN2P3, Villeurbanne, France
- <sup>6</sup> Centro de Aplicaciones Tecnológicas y Desarrollo Nuclear (CEADEN), Havana, Cuba
- <sup>7</sup> Centro de Investigaciones Energéticas Medioambientales y Tecnológicas (CIEMAT), Madrid, Spain
- <sup>8</sup> Centro de Investigación y de Estudios Avanzados (CINVESTAV), Mexico City and Mérida, Mexico
- <sup>9</sup> Centro Fermi – Centro Studi e Ricerche e Museo Storico della Fisica "Enrico Fermi", Rome, Italy
- <sup>10</sup> Chicago State University, Chicago, United States
- <sup>11</sup> Commissariat à l'Energie Atomique, IRFU, Saclay, France
- <sup>12</sup> Departamento de Física de Partículas and IGFAE, Universidad de Santiago de Compostela, Santiago de Compostela, Spain

- 13 Department of Physics Aligarh Muslim University, Aligarh, India
- 14 Department of Physics and Technology, University of Bergen, Bergen, Norway
- 15 Department of Physics, Ohio State University, Columbus, Ohio, United States
- 16 Department of Physics, Sejong University, Seoul, South Korea
- 17 Department of Physics, University of Oslo, Oslo, Norway
- 18 Dipartimento di Fisica dell'Università and Sezione INFN, Cagliari, Italy
- 19 Dipartimento di Fisica dell'Università and Sezione INFN, Padova, Italy
- 20 Dipartimento di Fisica dell'Università and Sezione INFN, Trieste, Italy
- 21 Dipartimento di Fisica dell'Università and Sezione INFN, Bologna, Italy
- 22 Dipartimento di Fisica dell'Università 'La Sapienza' and Sezione INFN, Rome, Italy
- 23 Dipartimento di Fisica e Astronomia dell'Università and Sezione INFN, Catania, Italy
- 24 Dipartimento di Fisica 'E.R. Caianiello' dell'Università and Gruppo Collegato INFN, Salerno, Italy
- 25 Dipartimento di Fisica Sperimentale dell'Università and Sezione INFN, Turin, Italy
- 26 Dipartimento di Scienze e Innovazione Tecnologica dell'Università del Piemonte Orientale and Gruppo Collegato INFN, Alessandria, Italy
- 27 Dipartimento Interateneo di Fisica 'M. Merlin' and Sezione INFN, Bari, Italy
- 28 Division of Experimental High Energy Physics, University of Lund, Lund, Sweden
- 29 European Organization for Nuclear Research (CERN), Geneva, Switzerland
- 30 Fachhochschule Köln, Köln, Germany
- 31 Faculty of Engineering, Bergen University College, Bergen, Norway
- 32 Faculty of Mathematics, Physics and Informatics, Comenius University, Bratislava, Slovakia
- 33 Faculty of Nuclear Sciences and Physical Engineering, Czech Technical University in Prague, Prague, Czech Republic
- 34 Faculty of Science, P.J. Šafárik University, Košice, Slovakia
- 35 Frankfurt Institute for Advanced Studies, Johann Wolfgang Goethe-Universität Frankfurt, Frankfurt, Germany
- 36 Gangneung-Wonju National University, Gangneung, South Korea
- 37 Helsinki Institute of Physics (HIP) and University of Jyväskylä, Jyväskylä, Finland
- 38 Hiroshima University, Hiroshima, Japan
- 39 Hua-Zhong Normal University, Wuhan, China
- 40 Indian Institute of Technology, Mumbai, India
- 41 Indian Institute of Technology Indore (IIT), Indore, India
- 42 Institut de Physique Nucléaire d'Orsay (IPNO), Université Paris-Sud, CNRS-IN2P3, Orsay, France
- 43 Institute for High Energy Physics, Protvino, Russia
- 44 Institute for Nuclear Research, Academy of Sciences, Moscow, Russia
- 45 Nikhef, National Institute for Subatomic Physics and Institute for Subatomic Physics of Utrecht University, Utrecht, Netherlands
- 46 Institute for Theoretical and Experimental Physics, Moscow, Russia
- 47 Institute of Experimental Physics, Slovak Academy of Sciences, Košice, Slovakia
- 48 Institute of Physics, Bhubaneswar, India
- 49 Institute of Physics, Academy of Sciences of the Czech Republic, Prague, Czech Republic
- 50 Institute of Space Sciences (ISS), Bucharest, Romania
- 51 Institut für Informatik, Johann Wolfgang Goethe-Universität Frankfurt, Frankfurt, Germany
- 52 Institut für Kernphysik, Johann Wolfgang Goethe-Universität Frankfurt, Frankfurt, Germany
- 53 Institut für Kernphysik, Technische Universität Darmstadt, Darmstadt, Germany
- 54 Institut für Kernphysik, Westfälische Wilhelms-Universität Münster, Münster, Germany
- 55 Instituto de Ciencias Nucleares, Universidad Nacional Autónoma de México, Mexico City, Mexico
- 56 Instituto de Física, Universidad Nacional Autónoma de México, Mexico City, Mexico
- 57 Institut of Theoretical Physics, University of Wrocław
- 58 Institut Pluridisciplinaire Hubert Curien (IPHC), Université de Strasbourg, CNRS-IN2P3, Strasbourg, France
- 59 Joint Institute for Nuclear Research (JINR), Dubna, Russia
- 60 KFKI Research Institute for Particle and Nuclear Physics, Hungarian Academy of Sciences, Budapest, Hungary
- 61 Kirchhoff-Institut für Physik, Ruprecht-Karls-Universität Heidelberg, Heidelberg, Germany
- 62 Korea Institute of Science and Technology Information, Daejeon, South Korea

- 63 Laboratoire de Physique Corpusculaire (LPC), Clermont Université, Université Blaise Pascal, CNRS-IN2P3, Clermont-Ferrand, France
- 64 Laboratoire de Physique Subatomique et de Cosmologie (LPSC), Université Joseph Fourier, CNRS-IN2P3, Institut Polytechnique de Grenoble, Grenoble, France
- 65 Laboratori Nazionali di Frascati, INFN, Frascati, Italy
- 66 Laboratori Nazionali di Legnaro, INFN, Legnaro, Italy
- 67 Lawrence Berkeley National Laboratory, Berkeley, California, United States
- 68 Lawrence Livermore National Laboratory, Livermore, California, United States
- 69 Moscow Engineering Physics Institute, Moscow, Russia
- 70 National Institute for Physics and Nuclear Engineering, Bucharest, Romania
- 71 Niels Bohr Institute, University of Copenhagen, Copenhagen, Denmark
- 72 Nikhef, National Institute for Subatomic Physics, Amsterdam, Netherlands
- 73 Nuclear Physics Institute, Academy of Sciences of the Czech Republic, Řež u Prahy, Czech Republic
- 74 Oak Ridge National Laboratory, Oak Ridge, Tennessee, United States
- 75 Petersburg Nuclear Physics Institute, Gatchina, Russia
- 76 Physics Department, Creighton University, Omaha, Nebraska, United States
- 77 Physics Department, Panjab University, Chandigarh, India
- 78 Physics Department, University of Athens, Athens, Greece
- 79 Physics Department, University of Cape Town, iThemba LABS, Cape Town, South Africa
- 80 Physics Department, University of Jammu, Jammu, India
- 81 Physics Department, University of Rajasthan, Jaipur, India
- 82 Physikalisches Institut, Ruprecht-Karls-Universität Heidelberg, Heidelberg, Germany
- 83 Purdue University, West Lafayette, Indiana, United States
- 84 Pusan National University, Pusan, South Korea
- 85 Research Division and ExtreMe Matter Institute EMMI, GSI Helmholtzzentrum für Schwerionenforschung, Darmstadt, Germany
- 86 Rudjer Bošković Institute, Zagreb, Croatia
- 87 Russian Federal Nuclear Center (VNIIEF), Sarov, Russia
- 88 Russian Research Centre Kurchatov Institute, Moscow, Russia
- 89 Saha Institute of Nuclear Physics, Kolkata, India
- 90 School of Physics and Astronomy, University of Birmingham, Birmingham, United Kingdom
- 91 Sección Física, Departamento de Ciencias, Pontificia Universidad Católica del Perú, Lima, Peru
- 92 Sezione INFN, Trieste, Italy
- 93 Sezione INFN, Padova, Italy
- 94 Sezione INFN, Turin, Italy
- 95 Sezione INFN, Rome, Italy
- 96 Sezione INFN, Cagliari, Italy
- 97 Sezione INFN, Bologna, Italy
- 98 Sezione INFN, Bari, Italy
- 99 Sezione INFN, Catania, Italy
- 100 Soltan Institute for Nuclear Studies, Warsaw, Poland
- 101 Nuclear Physics Group, STFC Daresbury Laboratory, Daresbury, United Kingdom
- 102 SUBATECH, Ecole des Mines de Nantes, Université de Nantes, CNRS-IN2P3, Nantes, France
- 103 Technical University of Split FESB, Split, Croatia
- 104 The Henryk Niewodniczanski Institute of Nuclear Physics, Polish Academy of Sciences, Cracow, Poland
- 105 The University of Texas at Austin, Physics Department, Austin, TX, United States
- 106 Universidad Autónoma de Sinaloa, Culiacán, Mexico
- 107 Universidade de São Paulo (USP), São Paulo, Brazil
- 108 Universidade Estadual de Campinas (UNICAMP), Campinas, Brazil
- 109 Université de Lyon, Université Lyon 1, CNRS-IN2P3, IPN-Lyon, Villeurbanne, France
- 110 University of Houston, Houston, Texas, United States
- 111 University of Technology and Austrian Academy of Sciences, Vienna, Austria
- 112 University of Tennessee, Knoxville, Tennessee, United States
- 113 University of Tokyo, Tokyo, Japan
- 114 University of Tsukuba, Tsukuba, Japan
- 115 Eberhard Karls Universität Tübingen, Tübingen, Germany

- <sup>116</sup> Variable Energy Cyclotron Centre, Kolkata, India
- <sup>117</sup> V. Fock Institute for Physics, St. Petersburg State University, St. Petersburg, Russia
- <sup>118</sup> Warsaw University of Technology, Warsaw, Poland
- <sup>119</sup> Wayne State University, Detroit, Michigan, United States
- <sup>120</sup> Yale University, New Haven, Connecticut, United States
- <sup>121</sup> Yerevan Physics Institute, Yerevan, Armenia
- <sup>122</sup> Yildiz Technical University, Istanbul, Turkey
- <sup>123</sup> Yonsei University, Seoul, South Korea
- <sup>124</sup> Zentrum für Technologietransfer und Telekommunikation (ZTT), Fachhochschule Worms, Worms, Germany